A $\delta^{11}B$ -pH calibration for the high-latitude foraminifera species Neogloboquadrina pachyderma and Neogloboquadrina incompta.

Elwyn de la Vega^{1*}, Markus Raitzsch², Gavin L. Foster³, Jelle Bijma⁴, Ulyssess Ninnemann⁵, Michal Kucera⁶, Tali L. Babila⁷, Jessica Crumpton Banks¹, Mohamed M. Ezat⁸, and Audrey Morley^{1,9*}.

10

15

20

Correspondence to: audrey.morley@universityofgalway.ie or elwyn.dlvega@gmail.com

Abstract. The boron isotopic composition of planktonic foraminifera is a powerful tool to reconstruct ocean pH 25 and CO₂ in the past. Applications to the high-latitude and polar oceans are however limited as robust calibrations between the δ^{11} B of foraminifera and ocean pH in these regions are lacking. Here, we present a new empirical calibration for the high latitude Arctic species Neogloboquadrina pachyderma and the sub-polar to temperate species Neogloboquadrina incompta using towed specimens from the Labrador Sea, Baffin Bay, and the Nordic Seas. When paired with in situ hydrographic data, this approach allows us to avoid key assumptions used in 30 traditional core top calibrations that are required to link shell geochemical composition to hydrographic conditions during their formation. We show that the foraminifera $\delta^{11}B$ of the species analysed is well correlated with the $\delta^{11}B$ of seawater borate ion. Further, the foraminiferal $\delta^{11}B$ values are consistently lower than seawater equilibrium borate values, consistent with the interpretation of more acidic seawater in the microenvironment due to 35 respiration. However, unlike published calibrations for non-spinose species to date the slope of the $\delta^{11}B$ foraminifera to $\delta^{11}B$ borate calibration is >1. We discuss several drivers of this higher sensitivity to pH and describe the possible role of vital effects in determining the boron isotopic composition of N. pachyderma and N.

¹ University of Galway, Ryan Institute, and School of Geography, Archaeology and Irish Studies, H91TK33 Galway, Ireland.

² Dettmer Group GmbH & Co. KG., 28195 Bremen, Germany

³ School of Ocean and Earth Science, University of Southampton, National Oceanography Centre Southampton, Southampton, SO14 3ZH, UK

⁴ Alfred-Wegener-Institut, Helmholtz-Zentrum für Polar- und Meeresforschung, Am Handelshafen 12, 27570, Bremerhaven, Germany

⁵ University of Bergen, Department of Earth Science and Bjerknes Centre for Climate Research, 5007, Bergen, Norway

⁶ MARUM - Center for Marine Environmental Sciences, University of Bremen, Bremen, Germany

⁷Case Western Reserve University, Department of Earth, Environmental and Planetary Sciences, Cleveland, Ohio, USA

⁸. iC3: Centre for ice, Cryosphere, Carbon and Climate, Department of Geosciences, UiT, The Arctic University of Norway, 9037 Tromsø, Norway

⁹ iCRAG – Irish Centre for Research in Applied Geosciences, Belfield, Dublin 4, Ireland.

incompta. Finally, we apply the tow calibration to core top samples from the Nordic Seas to validate the calibration for use in the paleorecord.

40 1 Introduction

45

50

55

60

65

The northern North Atlantic and the Southern Oceans are areas of strong vertical mixing and convection and as a result play a major role in air-sea gas exchange, including the release or storage of deep ocean CO₂ (Takahashi et al., 2009;Ezat et al., 2017;Shuttleworth et al., 2021). The North Atlantic, the Nordic Seas, the Labrador Sea, and Baffin Bay in particular are areas of deep-water formation and contribute to the formation of North Atlantic deep waters (NADW), a key component of the Atlantic Meridional Overturning Circulation (AMOC). Today, NADW ventilates 26% of the global deep ocean (Johnson, 2008) and carries dissolved CO₂ to depth making the Nordic and Labrador Seas major sinks of atmospheric CO₂. The extent to which CO₂ is taken out of the atmosphere in these regions is dependent on several factors including temperature, the strength of the AMOC (Schmittner and Galbraith, 2008), sea-ice extent (Rysgaard et al., 2009), and biological productivity (Raven and Falkowski, 1999). Understanding the variability and magnitude of changes in surface ocean pH and CO₂ fluxes in the high latitudes is critical to understand its contribution to regulate the ocean carbon cycle and global climate.

Whilst the knowledge of global atmospheric CO₂ over the last 800 kilo annum (ka) is known with confidence from bubbles of ancient air trapped in Antarctic ice cores (Bereiter et al., 2015), our understanding of regional oceanic CO₂ fluxes, their magnitude and temporal variability relies on marine CO₂ proxy records (e.g., Martínez-Botí et al., 2015; Shuttleworth et al., 2021; Si et al., 2024). One commonly applied proxy of marine CO₂ relies on the boron isotopic composition ($\delta^{11}B$) of foraminifera shells that tracks ocean pH (Cenozoic CO2 Proxy Integration Project Foster and Rae, 2016; Consortium et al., 2023). This proxy has been extensively applied at low and mid latitudes using species from cultures, tows, and core tops where their δ^{11} B-pH relationship has been well calibrated (Henehan et al., 2016;Raitzsch et al., 2018;Guillermic et al., 2020), and thoroughly tested against the CO₂ record from ice cores in areas where the ocean is in equilibrium with the atmosphere (Henehan et al., 2013; Chalk et al., 2017; de la Vega et al., 2023). However, reconstructing CO₂ at high latitudes is particularly challenging due to the lower species diversity living in areas of the surface ocean where temperature is <5°C and the lack of well constrained δ^{11} B calibrations in such species (Yu et al., 2013;Ezat et al., 2017). One such species is the non-spinose planktonic foraminifera Neogloboquadrina pachyderma. It is found in abundance at latitudes above 55-60°N and exclusively in surface waters colder than 4 °C. Considering these oceanographic regions are important areas of CO₂ uptake via NADW formation over the observational period, it is critical to constrain how the δ^{11} B in this species records changes in pH and CO₂.

Although the boron isotope system has a relatively well understood theoretical basis (e.g., Foster and Rae, 2016), calibrations are required to account for "vital effects" – offsets from the expected δ¹¹B value caused by foraminiferal physiology (e.g., Henehan et al., 2016; Hönisch et al., 2003). In general, geochemical calibrations rely on at least one of these three approaches: (1) the culturing of foraminifera in a controlled laboratory environment (e.g., Gray and Evans, 2019; Lea et al., 1999), (2) the collection of foraminifera from Holocene-aged core tops or sediment traps (e.g., Anand et al., 2003; Erez and Honjo, 1981; Dekens et al., 2002) and (3) the collection of living specimen using plankton tows (e.g., Martínez-Botí et al., 2011; Mortyn and Charles,

2003; Winkelbauer et al., 2023). Whilst the culturing approach has the merit of knowing the exact seawater chemistry in which the foraminifera grew, it doesn't fully represent the environment experienced in the open ocean, such as ontogenetic vertical migration (Meilland et al., 2021), changes in biological productivity, nutrient abundance, sea ice cover, or secondary diagenetic processes such as precipitation or dissolution in the water column and sediments. Culturing foraminifera is also a time consuming and specialist activity requiring ready access to live foraminifera and careful maintenance of culture conditions, which can be challenging. The approach using core top samples accounts for all secondary alterations of the primary signal as the foraminifera is incorporated in the sedimentary archive and is thus well-suited for application in the paleoclimatic record. However, it is challenged by the difficulty to find a natural modern range of upper ocean pH (reflected by the δ^{11} B of borate) that is sufficiently large to define a reliable calibration (e.g., Yu et al., 2013) and there remains considerable uncertainty in determining the seawater carbonate chemistry the foraminifera calcified in, especially in regions like the northern North Atlantic where there has been significant invasion of anthropogenic CO₂ (Yasunaka et al., 2023). Finally, there can be uncertainty in core top sample age making the determination of seawater temperature and anthropogenic carbon contribution more uncertaint.

To date, only one study has attempted to construct a δ^{11} B calibration (Yu et al., 2013) using *N. pachyderma* from core top samples from the Labrador and Irminger Sea covering a relatively narrow range of pH and assuming a constant habitat depth of 50 m. Several attempts have been made to constrain the habitat depth of *N. pachyderma* and it is often stated that this species is a subsurface dweller (e.g., Kohfeld et al., 1996;Simstich et al., 2003) that is migrating to deeper waters prior to calcifying a thick outer crust. However, more recent direct observations of *N. pachyderma* habitat across the Arctic and polar oceans show that the habitat depth of *N. pachyderma* is variable, can be shallow (i.e. < 20 m) and is primarily controlled by sea ice cover and chlorophyll intensity (Pados and Spielhagen, 2014;Greco et al., 2019) and not by diel vertical migration or the lunar phase (Greco et al., 2019). When sea-ice cover is reduced and/or when chlorophyll at the surface is low, the habitat generally deepens to 75–150 m (Greco et al., 2019). Critically, these studies have shown that heavily crusted *N. pachyderma* specimens can be found at any depth including the top 0-50 m (Tell et al., 2022) suggesting that there is no systematic ontogenetic vertical migration associated with reproduction or "crusting" for *N. pachyderma* (Manno and Pavlov, 2014;Tell et al., 2022). The considerable variability in habitat depth across the top 200 m of the surface ocean complicates the attribution of a single depth to core top calibrations and potentially results in large uncertainties when attributing modern pH and thereby δ^{11} B of borate to foraminiferal δ^{11} B.

To avoid the assumptions associated with traditional core top calibrations we present here a calibration using living N. pachyderma and N. incompta specimens (e.g., cytoplasm intact, no crust) collected via plankton tows from across a large range of pH in the Labrador Sea, Baffin Bay, and the Nordic Seas. This approach allows us to compare the foraminiferal $\delta^{11}B$ with the pH of seawater and hence $\delta^{11}B$ of seawater borate from the exact same depth at which the tows of N. pachyderma and N. incompta were collected. While this approach provides the most accurate hydrographic data for the calibration effort, the tow depth range, in some cases, integrates a large gradient in seawater carbonate chemistry and temperature, which introduces some uncertainties (reported in Table 2). We acknowledge that the depth of the plankton tows does not necessarily represent the depth of calcification. Further, the $\delta^{11}B$ composition of non-crusted specimens analysed here may be different to crusted specimen found in

marine climate archives. In order to assess the validity of the calibration we construct, we then apply the towbased calibration to a series of high latitude core tops alongside existing data from the literature to evaluate its application to the paleorecord.

Whilst *N. pachyderma* and *N. incompta* were historically considered as two morphotypes of the same species (*N. pachyderma* sinistral and dextral respectively), they are now considered two separate species based on genetics, biogeography and ecological distinctions (Darling et al., 2006;Cifelli, 1961). They are however closely related; both are non-spinose species and live in polar or subpolar environments. *N. pachyderma* is typically found in cold open ocean waters and is the only species present in waters below 4 °C (e.g., Baffin Bay, Labrador Sea, Greenland Sea) and *N. incompta* dominates warmer subpolar waters of the eastern Norwegian Seas, and subpolar North Atlantic. The large geographical area of the polar North Atlantic allows us to cover a wide range of temperature, convection and CO₂ flux, and as a result a large gradient of pH in this calibration.

2 Methods

130

135

140

145

150

155

2.1 Oceanographic setting

The dataset presented here was collected from the Nordic Seas, constituting the Greenland, Icelandic and Norwegian Seas (also sometimes called in conjunction with the Arctic Sea, the Arctic Mediterranean Sea), and the Labrador Seas. At the surface, the North Atlantic Drift enters the Nordic Seas (as "inflow") mainly through the Iceland-Scotland ridge, and to a lesser extent the Denmark Strait (Hansen and Østerhus, 2000;Østerhus et al., 2019). North of the Iceland-Scotland ridge the North Atlantic Drift becomes the Norwegian Current, a warm and saline current that gradually cools via air-sea exchanges as it flows northward. From the Arctic Ocean surface outflow through the Fram Strait feeds the East Greenland Current, and through the Canadian Archipelago the Baffin Island Current. Once in the Nordic Seas the East Greenland Current follows the Greenland coast and becomes the West Greenland Current entering the Labrador Seas and subsequently the Baffin Bay. This current partly mixes with the Irminger current, a branch of the North Atlantic Drift, which increases its salinity. Together, the West Greenland and Irminger Currents flow northward into the Baffin Bay before recirculating southward alongside the surface Labrador Current. The Arctic waters that enter the Baffin Bay through the Canadian Archipelago travel via various sounds and straits southward and are of surface and subsurface origin (Azetsu-Scott et al., 2010). Along the way they mix with low salinity waters from precipitation, river, and sea ice meltwater before contributing to the low-density Baffin Island Current on the Western margin of the bay. The Baffin Island Current then mixes with the outflow water from the Hudson Bay and merges with the Labrador Current.

This complex system of water masses influences seawater pH in all regions. Mainly, the cold waters of Arctic origins are characterized by low pH due to the strong temperature dependent solubility of CO₂ at lower temperatures. Conversely, the warmer and saline waters feeding the Norwegian margin, the Labrador Sea, and the southern part of the Baffin Bay are characterized by higher pH. These strong gradients in surface water pH also result in a large range of CO₂ offsets between the surface ocean and the atmosphere (Figure 1). As a result, this wide geographic spread and diversity in water masses allows for the large range of > 0.2 seawater pH (Table 2) and diverse foraminifera habitat included in this calibration effort.

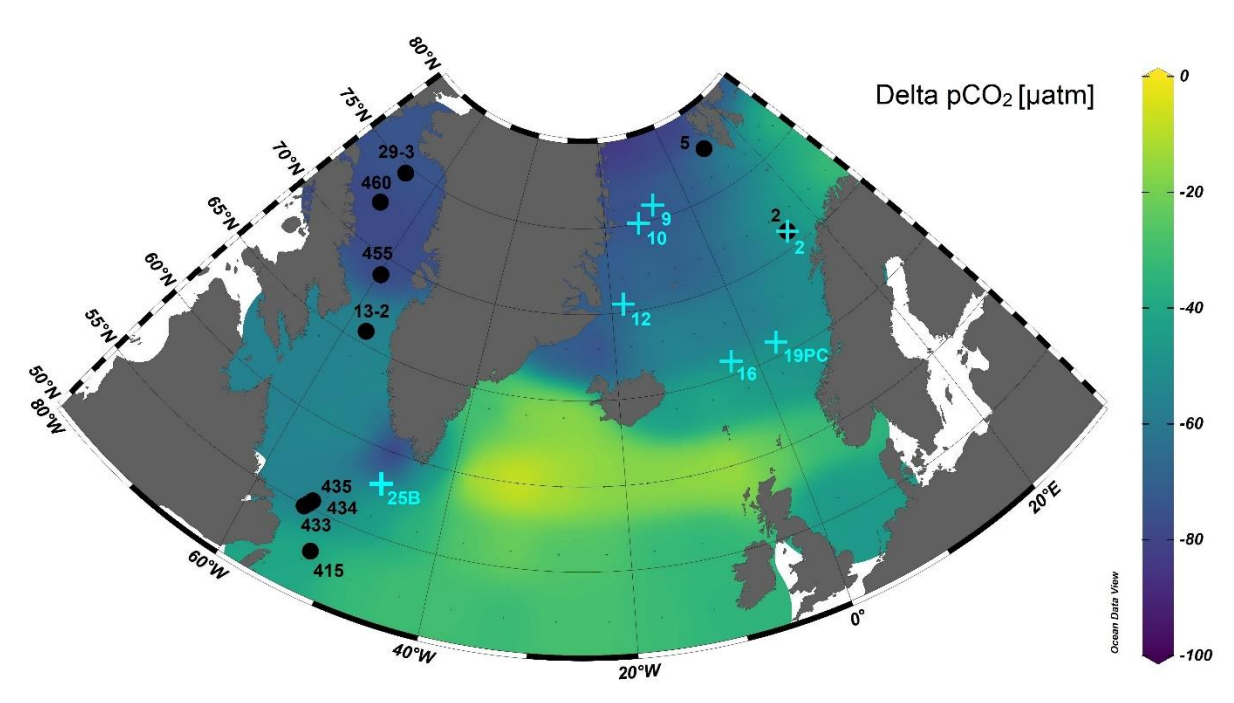


Figure 1. Map of the delta partial pressure of CO₂ (pCO₂, in units of micro atmospheres) defined as the difference between atmospheric and seawater pCO₂ (= pCO₂ atmosphere – pCO₂ seawater) at sea surface temperature (Takahashi et al., 2019) and location of stations where plankton tows (red circles) and core top samples (light blue crosses) were collected. Delta pCO₂ for the Baffin Bay was calculated using pCO₂ values reported in (Nickoloff et al., 2024). Map made with Ocean Data View (Schlitzer, 2002).

2.1. Sample material

160

165

170

175

180

Specimens collected via plankton tows include 15 N. pachyderma samples from the Labrador Sea and Baffin Bay collected during RV Maria S. Marian cruises MSM09 in 2008, MSM44 in 2015, and MSM66 in 2017. In addition, 5 tows containing N. incompta and 5 core top samples (containing N. pachyderma) were collected from the Nordic Seas during cruise CE20009 in August 2020 (Figure 1). Towed samples were collected from 100 µm mesh multinets, brought on board, and either immediately frozen at -80 °C or immediately picked into slides and frozen at -80 °C to preserve the foraminiferal cytoplasm. Frozen tows were thawed onshore and between 0.7 and 2 mg of uncrusted specimens with intact cytoplasm were hand-picked for $\delta^{11}B$ and trace elemental to calcium analysis. The average size fraction of tow samples from the Labrador Sea ranged between 182-248 µm determined using a Keyence HX 6000 digital microscope, however all specimen sizes available were included in analysis including specimen >100 and <300 μm to ensure enough material was available. Core tops were collected from multicores recovered during cruise CE20009 (September 2020) and cruise CAGE-ARCLIM (June 2022). The multicores were immediately processed onboard and sliced at 0.5 to 1 cm resolution, and subsequently frozen at -20 °C. On land, multicore tops were thawed or freeze-dried and wet-sieved at 63 µm. 1-2 mg of N. pachyderma were picked in the 200-250 µm size fraction. When possible morphotype II was favoured when picking specimens from core tops to minimize potential depth habitat variability with morphotypes following the classification of Altuna et al. (2018, Plate 1). All specimens from core tops were encrusted and while we selected specimens from a very narrow size fraction, we did not perform a systematic analysis of the degree of encrustation of N. pachyderma in the core top samples. Therefore, we cannot exclude that post-mortem depositional processes including the precipitation of inorganic calcite, dissolution, or recrystallization impact the thickness or geochemical composition of the crust as

the tests sink through the water column and settle at the seafloor. In Table S4 we list core tops that were radiocarbon dated. Accelerator mass spectrometry (AMS) radiocarbon (¹⁴C) was measured at the Keck Carbon Cycle Accelerator Mass Spectrometry facility at UC Irvine, USA. The samples for radiocarbon dating consist of the planktonic foraminifera *N. pachyderma*. Individuals were picked at from the 0.0-0.5cm interval for each core top (Table S4).

2.2. Estimates of δ^{11} B of borate

CTD (conductivity, temperature, depth) casts with Niskin bottles were deployed at each station for cruise CE20009 and water samples were collected for total alkalinity (TA) and dissolved inorganic carbon (DIC) analysis (described in Morley et al., 2024). This allows the carbonate chemistry of seawater to be fully constrained at exactly the same depth as where the tows were collected. $\delta^{11}B$ of borate was calculated from pH (derived from TA and DIC) and derived using the following equation:

$$\delta^{11} B_{B(OH)_{4}^{-}} = \frac{\delta^{11} B_{SW}[B]_{SW} - \epsilon_{\textit{B}}[B(OH)_{3}]}{[B(OH)_{4}^{-}] - \alpha_{B}[B(OH)_{3}]}) \text{ (eq. 1)}$$

Where the total boron in seawater $[B]_{sw} = 432.6 \times (salinity/35) \, \mu mol/kg$ (Lee et al., 2010), ϵ_B is the fractionation factor between the two boron species expressed as $\epsilon_B = (\alpha_B-1) \, x \, 1000$, the isotopic fractionation factor α_B between $B(OH)_3$ and $B(OH)_4$ is 1.0272 as determined by Klochko et al. (2006) and the $\delta^{11}B$ of seawater is 39.61 % (Foster et al., 2010). For stations in the Labrador Sea and the Baffin Bay the water chemistry was determined using nearby cruise data collected at the same time or the same month of the year as the tow samples (Table S3). For the towed samples, the $\delta^{11}B$ of borate was determined using the median of the hydrographic parameters within the towed sample depth interval.

205

210

215

220

200

185

190

195

For core top samples we estimate the depth of $\delta^{11}B$ of borate using the traditional core top approach to constrain calcification depth based on paired $\delta^{18}O$ measurements (e.g., Ravelo and Hillaire-Marcel, 2007). Briefly, we constrained calcification depth by projecting the $\delta^{18}O$ of N. pachyderma and N. incompta onto the equilibrium $\delta^{18}O$ of calcite in the water column ($\delta^{18}O_{\text{calcite.eq.PDB}}$) using modern hydrographic profiles and the paleotemperature equation derived by Shackleton (1974) as follow:

$$\delta^{18}O_{calcite.eq.PDB} = \delta^{18}O_{sw.SMOW} - (\frac{4.38 - \sqrt{4.38^2 - 4*0.1(16.9 - T)}}{0.2}) \text{ (eq. 2)}$$

Seawater temperature in degrees Celsius (T), $\delta^{18}O_{\text{calcite.eq.PDB}}$ is the equilibrium $\delta^{18}O$ of calcite on the PDB scale and $\delta^{18}O_{\text{sw.SMOW}}$ is the $\delta^{18}O$ of seawater on the SMOW scale (Table S1), either directly measured from CTD bottles or derived from salinity using the regional salinity– $\delta^{18}O_{\text{sw}}$ of Simstich et al. (2003). This approach yields a depth estimate for the core top foraminifera between 25 and 91 meters and an average of 65 meters (Morley et al., 2024, Supplementary Table 4). As in Morley et al. (2024) we did not apply a systematic correction for a vital effect on $\delta^{18}O$ values because there isn't consensus in the literature on the offset recorded in *N. pachyderma* collected from core top samples. Briefly, the negative $\delta^{18}O_c$ offset from equilibrium measured in living (uncrusted) *N. pachyderma* collected from plankton tows is highly variable within a region, across regions, seasons, and on interannual timescales (Stangeew, 2001; Volkmann and Mensch, 2001; Pados and Spielhagen, 2014; Livsey et al.,

2020). Furthermore, the addition of crust, typical for specimens recovered from core tops, increases the $\delta^{18}O_c$ signal because crust is isotopically heavier than ontogenetic calcite (Kozdon et al., 2009;Mikis et al., 2019). Variations in the degree of encrusting can therefore either "lower", completely "mask", or shift the vital effect towards positive values depending on the degree of encrustation (Kozdon et al., 2009). As a result, there remains considerable uncertainty in the exact value to use when correcting for the competing signals of vital effects and crust in *N. pachyderma*, with studies reporting both calcification in equilibrium (Jonkers et al., 2010;Jonkers et al., 2013;Mikis et al., 2019;Jonkers et al., 2022) and out of equilibrium with seawater (Kohfeld et al., 1996;Bauch et al., 1997;Simstich et al., 2003;King and Howard, 2005). By not applying a correction for vital effects or the contribution of crust calcite we avoid biasing calcification depth estimates towards deeper depths and lower $\delta^{11}B_{borate}$ values. This approach is also consistent with sediment trap studies from both the North and South Atlantic where $\delta^{18}O_c$ values measured on crusted *N. pachyderma* are in equilibrium with measured water column $\delta^{18}O$ (Jonkers et al., 2013;Mikis et al., 2019).

The pH and $\delta^{11}B_{borate}$ for core tops samples was calculated by applying a correction for anthropogenic carbon on DIC (using the anthropogenic DIC of GLODAPv2. 2016 ranging ~35 to 50 µmol/kg in the Nordic Sea stations in the upper 200 meters (Lauvset et al., 2022). For core tops dated with AMS radiocarbon dates younger than 550 years we did not apply a correction for anthropogenic carbon (Table S4). The uncertainty for calcification depth was defined as the minimum and maximum within a \pm 20-meter interval around the central value. We note that this approach yields an average depth of the foraminifera population signal, and that despite both species being observed to live throughout the upper 200 m of the water column (Greco et al., 2019), we assume the inferred depth is representative of where the majority of the population lives and calcifies. The $\delta^{11}B_{foram}$ and corresponding $\delta^{11}B_{borate}$ were fitted with a York regression (York et al., 2004) that accounts for the uncertainty in both the x and y axis.

245

225

230

235

240

2.3. Elemental and $\delta^{11}B$ analysis

Analysis was conducted in two laboratories at the University of Southampton (for samples from CE20009 in the Nordics Seas) and the Alfred Wagner Institute (AWI, for tows from the Labrador Sea and Baffin Bay). Standards and reference material are presented in both laboratories to showcase reproducibility.

250

255

260

2.3.1 Samples from cruise CE20009

Foraminifera from tows and core tops were cleaned using a modified version of the established foraminifera method to account for higher organic content in plankton tow samples (Henehan et al., 2016;Barker et al., 2003). All foraminifera were gently crushed between two glass slides to facilitate cleaning and clay removal was carried out through sequential Milli-Q rinses and brief ultrasonication to agitate the samples (core top samples only). Both core top and tow samples were oxidatively cleaned with a solution of H_2O_2 (30% by weight) buffered with 0.1M NH₄OH (3.4% of peroxide in the final oxidative mix). Samples were placed in a hot bath for 3x5 min for core tops and 3x20 min for tows to ensure the removal of additional organics, separated by brief 15-seconds ultrasonication. Samples were then weak acid-leached (in 0.0005 M HNO₃) for 30 seconds and dissolved in ~300 μ I of 0.15 M HNO₃. An aliquot of 20 μ I (diluted in 130 μ I 0.5 M HNO₃) was kept for elemental analysis, and the remainder kept for boron sample preparation and analysis.

Elemental analysis was performed on an Thermo Element Inductively Coupled Plasma Mass Spectrometer (ICP-MS) at Centre for Earth Research and Analysis Southampton (CERAS) at the University of Southampton and element-to-calcium ratios measured with ⁴³Ca and ⁴⁸Ca, then averaged, and referenced against in house mixed element standards. Bracketing standards were measured at the same concentration as samples. For samples bellow 1 mM, Element/Ca ratios typically drift, therefore, the concentration of the samples and standards were matched to account for this effect.El/Ca ratios measured included Mg and Ba. Based on the reproducibility of our in-house standards, the uncertainty for most elemental ratios is ~5 % (at 95 % confidence; (Henehan et al., 2015)). In order to showcase reproducibility between coretops measured at Southampton and tows at AWI (section 2.3.2), we report the long-term averages for Mg/Ca and Ba/Ca for NIST-C (coral reference standard) typically measured at Southampton, and the long-term average for JCP-1 typically measured at AWI and compare these to the interlaboratory assessment published in Stewart et al. (2021) and Hathorne et al. (2013), respectively (Table 1). This comparison shows that both laboratories produce consistent values without any significant interlaboratory offsets.

Table 1: Comparison of El/Ca standards measured at NOC and AWI

265

270

275

280

285

290

295

Standards	NIST-C		JCP-1 (uncleaned)		
El/Ca	Stewart et al. 2021	NOC	Hathorne et al. 2013	AWI	NOC (Stewart et al., 2016)
Mg/Ca	4.11±0.20	4.20±0.04	4.20±0.065	4.05±0.13	4.14±0.08
Ba/Ca	5.92±0.16	5.71±0.03	7.47±0.66	7.00±0.48	n/a

Samples for boron isotope analysis were first purified for boron by anion exchange chromatography in the boron-free class 100 laboratory of CERAS following the procedure of Foster (2008). A total procedure blank (TPB) was conducted for all batches of ~10 columns and ranged 31 to 92 pg (equivalent to 1-5% of the sample total boron). Samples were subsequently corrected using a long term $\delta^{11}B$ of TPB of -7.27 ‰ from long term measurement at the University of Southampton. This gave a $\delta^{11}B$ correction of 0.1 to 1.1 ‰. To test the effect of TPB correction on the regression slope, we present $\delta^{11}B$ both with and without TPB correction.

The purified sample was analysed for $\delta^{11}B$ at CERAS on a Thermo Neptune Multi Collector Inductively Coupled Plasma Mass Spectrometer (MC-ICPMS) with $10^{12} \Omega$ amplifier resistors, using a standard-bracketing technique with NIST SRM 951 (Foster, 2008;Foster et al., 2013). All other sample preparation and elemental analysis for the samples were conducted in the same CERAS laboratories at the University of Southampton.

The uncertainty on foraminifera $\delta^{11}B$ was empirically determined based on the uncertainty around the long-term measurement of JCp-1 Coral (Porites sp.) that has undergone the same chemical purification. The uncertainty is dependent on the boron content (Rae et al., 2011), i.e. the intensity of the ¹¹B signal of each sample. It is defined by the following equation (Anagnostou et al., 2019):

$$2\sigma = 12960e^{-212 \times [11B]} + 0.3385e^{-1.544 \times [11B]}$$
, (eq. 3)

where [^{11}B] is the intensity of $\delta^{11}B$ signal in volts. Carbonate and boric acid samples were measured at CERAS and AWI and are in good agreement. The long-term $\delta^{11}B$ of JCp-1, AE120 and AE121 at CERAS are (at 1σ)

24.21 \pm 0.12‰, -20.2 \pm 0.19‰ and 19.59 \pm 0.28‰ respectively, in good agreement with results of Gutjahr et al. (2021) and Stewart et al. (2021), and are comparable with values measured at AWI of 24.28 \pm 0.3‰ (Raitzsch et al., 2018), -19.85 \pm 1.57‰ (n=4) and 19.5 \pm 0.79‰ (n=10), respectively. Samples with substantial TPB corrections have lower confidence due to higher uncertainty in the $\delta^{11}B$ of TPB samples (given the low boron content). Applying a long term $\delta^{11}B$ of TPB of -7.27 ‰ may not be representative of the true value. As a result, for samples with substantial TPB correction, the uncertainty of $\delta^{11}B_{TPB}$ was propagated into the corrected $\delta^{11}B$ value measured on foraminifera samples (e.g., $\delta^{11}B_{foram}$).

2.3.2. Samples from the Labrador Sea and Baffin Bay

300

305

310

315

320

325

330

335

Boron (B) isotope ratios for samples from the Labrador Sea were measured following Raitzsch et al. (2018). Briefly, the cleaned samples were dissolved in $60 \,\mu\text{L}$ of $1 \,\text{N}$ HNO₃ and loaded on a Savillex teflon lid then closed and turned upside to be micro-distilled on a hotplate to separate boron from the carbonate matrix. The micro-distillation method in Ca-rich matrix samples such as foraminifera yields a B recovery of ~100 %, a low procedural blank, and accurate results, even at low B concentrations (Gaillardet et al., 2001;Wang et al., 2010;Misra et al., 2014;Raitzsch et al., 2018). The procedural blank contribution during this study was $10 - 50 \,\text{pg}$ B, which equates to ~0.2 %–0.8 % of the total [B] in the micro-distillation vial. The distillate containing only boron was diluted with 2% HNO₃ and analysed for boron isotopic composition in triplicate using a Nu Plasma II multi-collector inductively coupled plasma mass spectrometry (ICPMS) at AWI (Bremerhaven, Germany) that is equipped with a customized detector array of 16 Faraday cups and 6 secondary electron multipliers (SEM), also termed ion counters (IC), where high-mass IC5 was used for ^{11}B and IC0 for ^{10}B .

A standard-sample-bracketing technique was used to correct for the instrumental mass bias and drift using the boron reference material NBS 951 and frequent analysis of control standard AE121 with an isotopic composition similar to that of foraminifera was monitored to ensure measurement accuracy. Each micro-distilled sample was analysed in triplicate where at least two measurements were used for averaging the $\delta^{11}B$ value measured. Measurement uncertainties are reported as 2 standard deviations (2σ) derived from triplicate measurements or as \pm 0.30 % determined from long-term reproducibility (2σ) of the control standard, whichever is larger. For elemental to calcium (El/Ca) ratios the Labrador Sea and Baffin Bay samples were analysed using a Nu AttoM high-resolution double-focusing inductively coupled plasma mass spectrometer (ICP-MS) at the AWI.

2.4. Core top samples

To evaluate the validity of the tow-based δ^{11} B-pH calibration the core tops were considered as unknown paleo samples by applying the calibration equation derived from the plankton tows together with the revised Mg/Ca temperature calibration recently published by Morley et al. (2024). We applied this scheme to core tops from various location in the North Atlantic, cruise CE20009 and CAGE-ARCLIM (Nordic seas, this study), RAPID-35-25B (North Atlantic, (Yu et al., 2013;Moffa-Sánchez et al., 2014)), and JM-FI-19PC (Norwegian sea, (Ezat et al., 2017)). The foraminiferal δ^{11} B data from Ezat et al. (2017) measured with negative thermal ionization mass spectrometry (N-TIMS) was corrected for offsets in analytical techniques (using a correction of -1‰ defined by the foraminifera data of Farmer et al. (2016) to align with our data sets measured with MC-ICPMS. We calculate δ^{11} B-derived pH (eq 1.) and atmospheric CO₂ and correct for CO₂ differences between foraminifera habitat depth

and sea surface (from CTD or GLODAP v2 pCO₂ profiles) as well as local air-sea CO₂ disequilibrium (Takahashi et al., 2019), and compare our result to the ice core CO₂ record (Bereiter et al., 2015) over the last 500 years. Unlike comparing foraminiferal $\delta^{11}B$ core top values to modern pH and $\delta^{11}B$ borate which does not account for possible sediment age variations, this approach allows for: (1) comparison of $\delta^{11}B$ -derived CO₂ with an independent record from the ice core; and (2) the knowledge of CO₂ variations in the recent past to evaluate the range of CO₂ (and pH) possibly recorded by the $\delta^{11}B$ of core top foraminifera of variable ages.

For this calculation we use the constant fractionation factor determined by Klochko et al. (2006); eq. 1). We use a δ^{11} B of seawater of 39.61 ‰ (Foster et al., 2010), and use alkalinity as a second carbonate parameter in the CO₂ calculation (Zeebe and Wolf-Gladrow, 2001). Aqueous CO₂ was determined as follow:

$$CO_2 = \frac{{}^{TA} - \frac{K_B \cdot B_T}{K_B + [H^+]} - \frac{K_W}{[H^+]} + [H^+]}{\frac{K_1}{[H^+]} + \frac{2K_1 K_2}{[H^+]^2}}$$
(eq. 4)

TA is the total alkalinity measured from CTD bottle profiles. To account for uncertainty in habitat depth TA uncertainty was estimated by integrating the total range of TA within the upper 100 meters of the water column. K_B is the equilibrium constant of boron species in seawater (a function of temperature T, salinity S and pressure P, (Dickson, 1990)), B_T the concentration of boron in seawater (432.6 μ mol kg⁻¹, (Lee et al., 2010), [H⁺] the concentration of H⁺ determined from pH = $-\log[H^+]$ (total scale), K_w the dissociation constant of water (function of T, S and P), and K_1 and K_2 the first and second dissociation constants of carbonic acid (function of T, S and P, (Sulpis et al., 2020)). The partial pressure of pCO₂ (in parts per million, ppm) is determined as:

$$p\mathrm{CO}_2 = [\mathrm{CO}_2]_\mathrm{sw} \! / \! K_0$$

With $[CO_2]_{sw}$, the aqueous CO_2 concentration (eq. 4), and K_0 Henry's law constant (Weiss, 1974). Following Martínez-Botí et al. (2015) and Chalk et al. (2017), the p CO_2 uncertainty was determined with a Monte Carlo simulation (10,000 realisations) to account for the uncertainty of all input parameters (all with a normal distribution). An error envelope was calculated at 1 and 2 σ based on the 68% and 95% distribution of all the realisations.

3-Results

340

345

350

355

360

365

370

3.1 Tow samples

The $\delta^{11}B$ of towed *N. pachyderma* and *N. incompta* samples from the Labrador and Nordic Sea (i.e. $\delta^{11}B_{foram}$) are compared to seawater $\delta^{11}B$ borate (e.g., $\delta^{11}B_{borate}$) in Figure 2a. The $\delta^{11}B_{foram}$ of both species overlaps and both are offset to lower $\delta^{11}B$ than ambient borate. The regression for these data, using a constant α_B (Klochko et al., 2006) is best described by the following equation (with 1σ uncertainty, Figure 2a, Table 3), with a mean square weighted deviation (mswd) of 0.58 (and p=0.28):

$$\delta^{11}B_{foram.} = 1.58 (\pm 0.38) * \delta^{11}B_{borate} - 11.09 (\pm 5.9) (n=16)$$

The slope of 1.58, being larger than unity, shows that at lower ambient δ¹¹B_{borate} (lower pH), the δ¹¹B_{foram} is more offset from equilibrium than at higher δ¹¹B_{borate}. Furthermore, the slope lies below the 1:1 δ¹¹B_{foram}: δ¹¹B_{borate} line. When assessing *N. pachyderma* samples by themselves (i.e. tows from the Labrador Sea) the slope is steeper at 1.82. However, both slopes and intercepts are within error of each other (Table 3). We do not attempt to define a slope for *N. incompta*-only due to the narrow range of pH and δ¹¹B_{borate} covered for these samples. The effect of TPB correction on δ¹¹B and the regression slope (Supplementary Figure S1, Table S2) shows that the slope remains >1 when samples with high TPB are not included in the regression (Figure S1b) or not TPB corrected (Figure S1c). Elemental data Ba/Ca of *N. pachyderma* and *N. incompta* show highly variable values ranging 2 to 602 μmol/mol (Figure 4, Table 2).

Region	Cruise	Station	Tow depth Species	Species	Depth	표	_	DIC	TA :		Temp Sal		δ^{11} B _{bor}		ю	δ^{11} B _{foram}		Ba/Ca
	OI	ID	[m]		[m] 10	_	10	ш́т]	[µmol.kg 1]	[%]		[nsd]	[‰] er	err (lw) err	err (up) [9	[‰] ei	rr (±)	[µmol.mol ⁻¹]
NE Norwegian Sea	CE20009	2a	0-10	N.incompta	2	5	8.14	NA	2068 2	2294	10.7	34.44	17.12	0.29	0.29 1	15.01*	2.00	601.80
	CE20009	2b	10-20	N.incompta	15	2	8.16	NA	2066 2	2305	10.6	34.63	17.37	0.04	0.04	15.61*	2.00	525.70
	CE20009	2c	20-30	N.incompta	25	5	8.16	NA	2073 2	2308	10.2	34.80	17.29	0.04	0.04	14.8*	2.00	530.80
Fram Strait	CE20009	5	0-40	N.incompta	20	20	8.14	NA 2	2118 2	2320	7.5	34.90	16.80	0.56	0.33 1	15.34*	2.00	328.70
Davis Strait	MSM44	GeoB19913-2	0-100	N.pachyderma	20	20	8.12 0.0	0.009	2059 2	2217	0.1	32.48	15.70	0.40	0.10	14.04	06.0	2.97
	MSM44	GeoB19913-2	100-200	N.pachyderma	150	20	8.04 0.0	0.033	2130 2	2246	-1.2	33.51	15.13	0.15	0.10	13.00	0.82	2.93
Northern Baffin Bay	MSM44	GeoB19929-3	80-100	N.pachyderma	06	10	8.00 0.0	0.001	2146 2	2240	-1.1	33.76	14.89	0.02	0.10	11.59	1.15	2.05
	MSM44	GeoB19929-3	100-200	N.pachyderma	150	20	7.95 0.0	0.024	2156 2	2239	-0.7	33.94	14.67	0.15	0.10	12.21	0.97	2.02
Southern Baffin Bay	MSM09/2	GeoB455	80-100	N.pachyderma	06	10	8.05 0.0	0.009	2127 2	2243	-1.1	33.54	15.20	0.11	0.10	11.76	0.87	2.90
Southern Labrador	MSM09/2	GeoB415	20-40	N.pachyderma	30	10	8.11 0.0	0.005	2061 2	2199	1.5	32.23	15.79	0.02	0:30	13.05	0.51	10.46
Sea	MSM09/2	GeoB415	40-60	N.pachyderma	20	10	8.09 0.0	0.016	2098 2	2219	-0.7	33.30	15.48	0.02	0.30	13.38	0.48	20.63
Labrador Sea	MSM09/2 GeoB433	GeoB433	100-150	N.pachyderma	125	25	8.01 0.0	0.010	2195 2	2239	4	34.70	15.48	0.02	0:30	13.74	0.38	17.18
	MSM09/2	GeoB434	0-20	N.pachyderma	10	10	8.05 0.0	0.001	2035 2	2199	8.8	33.31	16.08	0.02	0.30	14.11	0.51	15.00
	MSM09/2	GeoB434	20-40	N.pachyderma	30	10	8.12 0.0	0.006	2068 2	2241	4.8	33.79	16.28	0.02	0.30	14.62	0.55	20.80
	MSM09/2	GeoB435	100-150	N.pachyderma	125	25	8.04 0.0	0.000	2147 2	2291	4.1	34.70	15.65	0.02	0:30	13.86	0.17	6.46
Baffin Bay	MSM09/2	GeoB460	40-60	N.pachyderma	20	10	8.08 0.0	0.004	2145 2	2261	-1.4	33.07	15.33	0:30	0:30	12.82	98.0	9.44

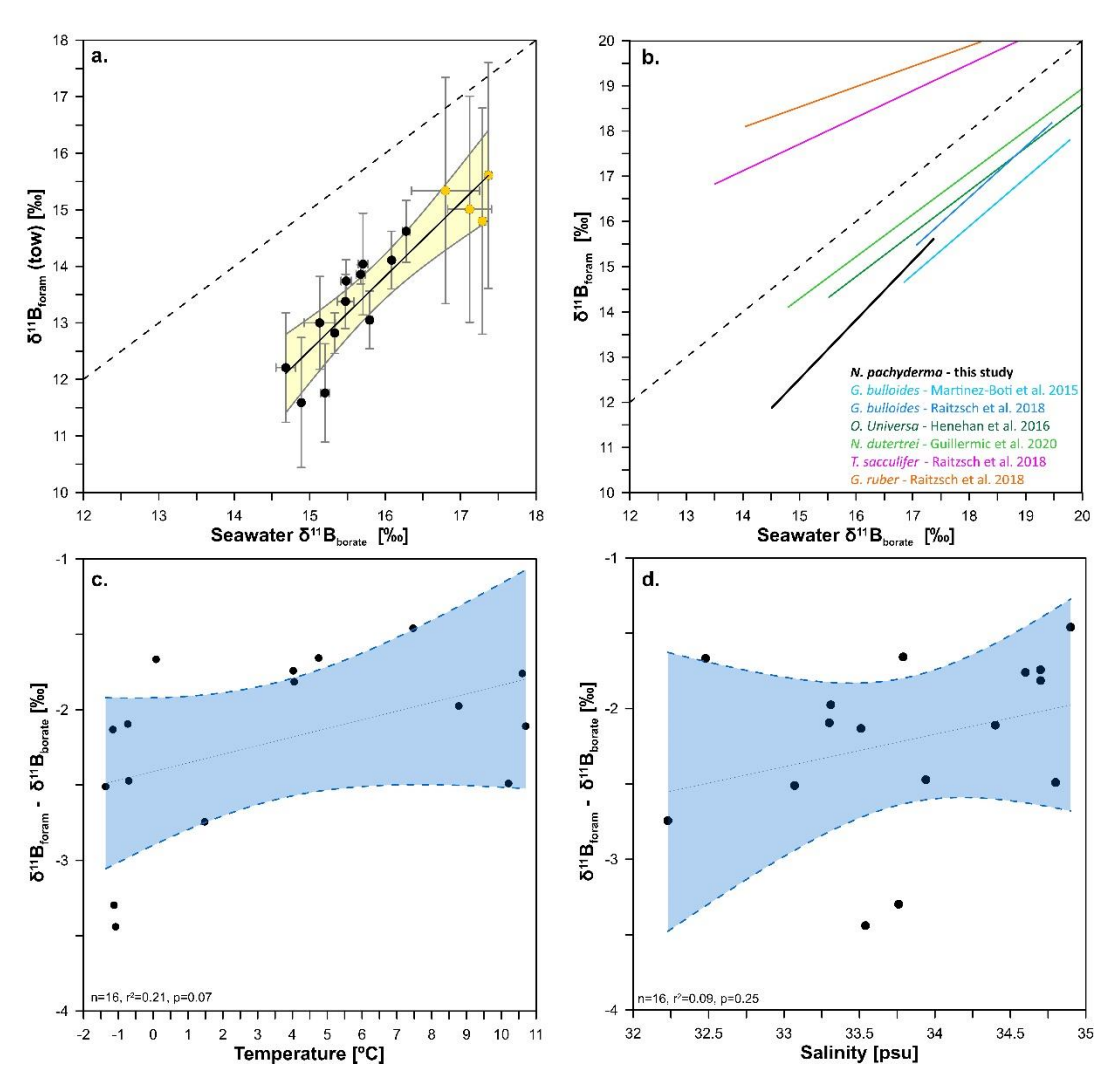


Figure 2. Relationship between the $\delta^{11}B$ of towed *N. pachyderma* (black circles) and *N. incompta* (yellow circles) with the $\delta^{11}B$ of seawater borate. Panel **a** shows $\delta^{11}B$ of towed specimens against $\delta^{11}B$ of seawater borate without a temperature correction on α_B on the calculation of $\delta^{11}B$ of borate. We fitted the data with a York regression (black line) and a 95% confidence envelope (light yellow shade), the x and y error bars represent the borate $\delta^{11}B$ uncertainty and the foraminifera $\delta^{11}B$ external uncertainty (see methods). The 1:1 line is shown by the black dashed line. Panel **b** shows calibration equations for other planktonic foraminifera next to the tow-based calibration equation derived here for *N. pachyderma*. Panels **c** and **d** show the regression between $\delta^{11}B_{\text{foram}}$ - $\delta^{11}B_{\text{borate}}$ offset and temperature (n=16, p=0.07, r²=0.22) and salinity (n=16, p=0.25, r²=0.10) respectively. The blue envelope represents the 95% confidence interval of the linear regression.

Table 3. Boron Isotope Calibration equation for *N. pachyderma* and *N. incompta*, and corresponding mean squared weighted deviation (mswd).

Sample Type	Slope($\pm 1\sigma$)	Intercept($\pm 1\sigma$)	mswd
Tows (N. pachyderma + N. incompta)	$1.58(\pm 0.38)$	-11.09(±5.9)	0.58
Tows (N. pachyderma only)	$1.82(\pm 0.5)$	-14.95(±7.77)	0.58

3.2. Relationship between δ^{11} B, temperature and salinity.

390

395

The foraminifera δ^{11} B exhibit a significant correlation with temperature (Fig S2 S1, r^2 = 0.58, p<<0.05) and salinity (Fig.S2, r^2 = 0.24, p= 0.017), which is likely due to covariance between carbonate system parameters, temperature, and salinity. To evaluate the influence of temperature and salinity on the proxy system we plot them against the

offset between $\delta^{11}B_{\text{foram}}$ and predicted $\delta^{11}B_{\text{borate}}$ (Figures 2c and 2d) and in both cases the correlation is not significant (i.e. p<0.05).

405 3.3. Applying the calibration to core top samples.

Whilst tows provide information about the original signal imprinted in well constrained calcifying environments, the application in the paleorecord relies on sediment samples with foraminifera that incorporate the calcification depth during ontogeny and post depositional environment processes in terms of sedimentation rate, corrosiveness of porewaters etc. The tow-based foraminifera $\delta^{11}B$ calibration equation based on temperatures calculated from the Mg/Ca- $\delta^{18}O$ correction scheme (Morley et al., 2024) yields reconstructed atmospheric pCO₂ concentrations that span the pre-industrial (280 ppm) to modern range (420 ppm)

4 Discussion

410

N. pachyderma and N. incompta are both non-spinose asymbiotic genetically sister species inhabiting the high latitude oceans (Darling et al., 2006). While their geographic distribution in the North Atlantic overlaps slightly at temperatures between 6-10 °C (Darling et al., 2006) each species inhabits distinct environmental conditions: warm Atlantic waters at subpolar latitudes of high pH for N. incompta, and cold polar waters of lower pH for N. pachyderma. Combining them in our study therefore allows us to cover a wider range of pH, and hence δ¹¹B_{borate}, improving the overall calibration. The minor difference in the calibration slopes when considering N. pachyderma alone or if both species are combined (Table 3) further support this approach.

4.1. Potential drivers of δ^{11} B sensitivity and alteration of microenvironment.

Our new calibration shows that the δ¹¹B_{foram} recorded by *N. pachyderma* and *N. incompta* is lower than the δ¹¹B of seawater borate (1:1 line, Figure 2). This result is in agreement with other published calibrations of the non-spinose species, *Globoconella inflata*, the symbiont-bearing spinose species *O. universa* (Henehan et al., 2016), and the symbiont-barren spinose species *G. bulloides* (Martínez-Botí et al., 2015). Further we observe that the slope of the regression is >1 (Figure 4e, Table 3). This observation contrasts with previously published δ¹¹B calibrations that show either a slope close to unity in line with the expected pH sensitivity from δ¹¹B of borate in seawater such as that found for epifaunal benthic foraminifera (Rae et al., 2011), *G. bulloides* (Martínez-Botí et al., 2015), *O. universa* (Henehan et al., 2016) and corals *Desmophyllum dianthus* (Anagnostou et al., 2012;McCulloch et al., 2012) and *Balanophyllia elegans* (Gagnon et al., 2021), or a slope <1 like the spinose symbiont-bearing species *G. ruber* (Henehan et al., 2013) and *T. sacculifer* (Sanyal et al., 2001;Martínez-Botí et al., 2015).

Interpretations of a weaker sensitivity (i.e. slope <1) to pH for *G. ruber* and *T. sacculifer* invoke photosymbiont activity, calcification and/or foraminifera metabolism, altering the pH of the diffusion-controlled microenvironment immediately surrounding the living foraminifera (e.g. (Henehan et al., 2016; Hönisch et al., 2003; Zeebe et al., 2003). In this scenario, lower pH in the microenvironment relative to ambient seawater immediately surrounding *N. pachyderma* and *N. incompta* specimens could arise from the CO₂ flux from foraminiferal respiration and calcification, which is offset/compensated for by CO₂ drawdown by symbionts in

440 the photosymbiont bearing spinose foraminifera (Zeebe et al., 1999;Rink et al., 1998). Alternative explanations for the patterns seen in photosymbiont bearing foraminifera invoke the incorporation of the isotopically heavy B(OH)₃ at slower calcification rates at lower pH, suggested to increase $\delta^{11}B_{foram}$ resulting in a shallow $\delta^{11}B_{foram}$ – $\delta^{11}B_{borate}$ slope (Uchikawa et al., 2015; Farmer et al., 2019). Whether or not calcification rates impact $\delta^{11}B_{foram}$ in N. pachyderma in this way remains to be determined because little is known about the exact foraminiferal 445 calcification rates in their natural environment. Inferred calcification rates based on laboratory culturing experiments and temperature dependent modelling suggest that Neogloboquadrinoids have lower calcification rates overall than other planktonic foraminifera species (Lombard et al., 2011). Furthermore, recent advances in three-dimensional imaging techniques (microCT scans) propose that growth patterns of Neogloboquadrinoids through ontogeny follow a distinct growth trajectory that unlike other spinose species slows at maturity for the final whorl of chambers (Burke et al., 2020), which constitute 70% or more of the total pre-gametogenic CaCO₃. 450 Whole-shell measurements of non-crusted tows, such as those here, are likely dominated by the isotopic composition recorded in these terminal chambers. In this scenario, if boric acid incorporation at low pH is responsible for <1 slopes in some species of foraminifera, it is unlikely to play a role in the Neogloboquadrinoids data presented here as low growth rates are associated with elevated $\delta^{11}B$ above borate rather than below borate 455 (Figure 2b; (Farmer et al., 2019; Uchikawa et al., 2015)).

In the following sections we explore additional mechanisms that could explain the lower-than-expected δ^{11} B_{foram} values and high sensitivity of *N. pachyderma* to low seawater borate (slope <1).

4.1.1. Foraminiferal microenvironment and calcification

465

470

Non-spinose foraminifera are generally devoid of photosynthetic symbionts; the pH of the micro-environment around such foraminifera is expected to more acidic than the ambient seawater. The respiration and calcification of foraminifera both release CO₂ into the microenvironment during these processes, which have been suggested as the main drivers explaining the lower-than-expected δ¹¹B_{foram} values in symbiont-barren species (Foster, 2008;Hönisch et al., 2003;Martínez-Botí et al., 2015;Yu et al., 2013).

To assess the calcification environment for N. pachyderma we estimated microenvironmental pH and the calcite saturation state (Ω_{calcite}) for our plankton tow dataset. Briefly, we derived Ω_{calcite} at calcification depth using hydrographic profiles (TA and DIC) which yields on average $\Omega_{\text{calcite}} = 2.2$. One way to approximate the conditions within the micro-environment of a living foraminiferal, without turning to complex diffusion-reaction modelling (e.g., Zeebe et al., 2003), is to simply model the effect of removing TA and DIC in a 2:1 ratio to simulate the influence of calcification (c.f. Hönisch et al., 2019). Following Hönisch et al. (2019) we modelled the progressive removal of up to 200 and 400 μ mol kg⁻¹ from the ambient DIC and TA, respectively (as in Hönisch et al., 2019; Figure 3). We caveat that this decrease in DIC and TA may be counteracted by diffusion. Taking the δ^{11} B values of the N. pachyderma and N. incompta at face value, this treatment implies an average pH of 7.4 in the microenvironment with $\Omega_{\text{calcite}} = 0.4$. This suggests that N. pachyderma calcifies in waters undersaturated with respect to calcite.

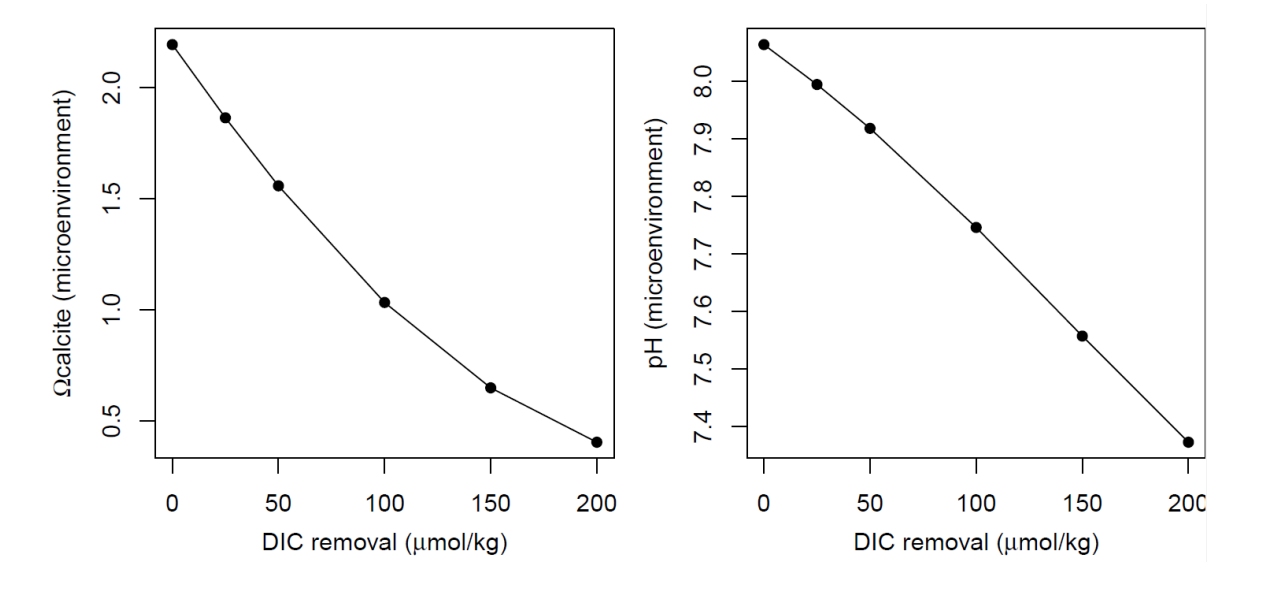


Figure 3. Theoretical effect of calcification (inducing a decrease of TA:DIC in a 2:1 ratio) on the Omega calcite and pH of seawater in the foraminifera microenvironment,

Calcification in foraminifera, like in many marine carbonates (Gilbert et al., 2022), takes place in an internal space within a fluid, the calcifying fluid, that is ultimately modified from ambient seawater carbonate chemistry (de Nooijer et al., 2014 and references therein). Benthic foraminifera have been observed to upregulate the pH in their calcifying fluid as high as 9 (de Nooijer et al., 2009) by the removal of protons via a Ca-ATPase enzymatic pump (Toyofuku et al., 2017) and/or alkalinity elevation of seawater vacuoles to facilitate calcification (Bentov et al., 2009). It is likely that DIC is also elevated in the calcifying fluid by passive CO₂ diffusion and active HCO₃-pumping (Ujiié et al., 2023). Indeed, genes relating to these processes were recently identified in foraminifera by Ujiié et al. (2023).

Whether or not *N. pachyderma* upregulates its internal pH remains to be determined, however, active proton pumping as a mechanism for *N. pachyderma* calcification aligns well with the recent biomineralization model proposed for Mg incorporation in *N. pachyderma* outlined in Morley et al. (2024). Briefly, they demonstrated that the preferential exclusion of Mg²⁺ into *N. pachyderma* is compromised in unfavourable calcification environments (e.g., at low seawater [CO₃²⁻] and SST >5 °C) in order to maintain energy for proton removal (see also (Evans et al., 2018;Zeebe and Sanyal, 2002). This observation invokes two important processes: (1) the generation and transport of bicarbonate and protons across the calcifying membrane and (2) that proton pumping may be less efficient for *N. pachyderma* at temperatures below 5 °C and low sea water [CO₃²⁻]. The latter process may provide an explanation for the steep δ^{11} B_{foram}: δ^{11} B_{borate} slope observed here in equation 1, considering that the samples collected from the coldest and most acidic environments lead to the largest offset from a slope = 1 (Figure 2c).

Assuming *N. pachyderma* upregulate their internal pH, the lower-than-expected $\delta^{11}B_{foram}$ values, suggesting a calcification fluid that is undersaturated with respect to calcite, remain puzzling. Following Gagnon et al. (2021) these observations could be reconciled if we consider boric acid diffusion into the calcifying fluid as part of the biomineralization process. If the diffusion of boric acid between the calcifying fluid and the microenvironment around the foraminifera is fast, while the exchange of seawater between the two is slow, it is possible for the concentration of boric acid internally to be the same as that in the micro-environment. Since the $\delta^{11}B$ of each

aqueous boron species is set by their relative proportions, this sets the $\delta^{11}B$ of borate in the calcifying fluid to be equal to the $\delta^{11}B$ of borate externally, even if the pH internally is significantly greater than the micro-environment. While this model reconciles the upregulation of pH in the calcifying fluid enabling calcification with $\delta^{11}B_{foram}$ values representative of the (undersaturated) microenvironment surrounding the foraminifera, it awaits direct determination of the calcifying fluid pH in *N. pachyderma* to validate it.

4.1.2 The effect and impact of temperature on the boron isotope fractionation factor α_B

The influence of temperature on the aqueous boron isotope fractionation factor α_B has been the subject of debate (Hönisch et al., 2019) even though there is a theoretical thermodynamic basis for α_B to be influenced by temperature (Zeebe, 2005), its magnitude is uncertain and it has not been conclusively demonstrated experimentally. So far, the fractionation α_B has been determined at 25 and 40 °C at a salinity of 35 (Klochko et al., 2006). However, large uncertainties prevent a conclusive quantification of the temperature dependence of α_B , which has been used to argue against a significant temperature sensitivity of α_B over the temperature range used in most $\delta^{11}B$ -pH calibrations and paleo-pH studies (Foster and Rae, 2016). In Figure 2, we show the calibration equation with constant α_B as defined in Klochko et al. (2006) and in Figure S2c with a temperature dependent α_B as defined in Hönisch et al. (2019).

Due to the large temperature gradient in our dataset, α_B corrected for temperature has a significant effect on the slope and intercept (Figure S2b and S2c). Like in other symbiont-barren planktonic foraminifera the temperature correction, when applied to *N. pachyderma*, reduces the large negative offset between $\delta^{11}B_{foram}$ and predicted $\delta^{11}B_{borate}$ however the microenvironmental pH remains slightly below the predicted $\delta^{11}B_{foram}$: $\delta^{11}B_{borate}$ line. Therefore, even with a temperature dependent α_B *N. pachyderma* would still require manipulation of microenvironmental pH to reconcile the disequilibrium isotopic offset from seawater values. Furthermore, there is no significant correlation between the offsets of *N. pachyderma* $\delta^{11}B$ from $\delta^{11}B_{borate}$, and temperature (Figure 2c), arguing against a strong influence of a temperature dependent α_B . Thus, although a temperature dependence on the fractionation factor is likely to exist, our data suggests that it is not significant over the temperature range relevant for *N. pachyderma*.

4.2. The marine aggregate habitat hypothesis.

505

510

515

520

525

530

535

It has been recently suggested that some non-spinose foraminifera live in marine aggregate (also referred to as marine snow or particulate organic matter). This has been indirectly observed in laboratory culture for *N. pachyderma* (Davis et al., 2020), *G. truncatulinoides* (Richey et al., 2022) and from plankton net for *G. menardii* and *N. dutertrei* (Fehrenbacher et al., 2018). Geochemical analysis of the shells of these species tend to show elevated Ba/Ca (Fehrenbacher et al., 2018;Richey et al., 2022;Fritz-Endres et al., 2022;Hupp and Fehrenbacher, 2023) compared to species that have not been observed in marine aggregates, and well above Ba/Ca values expected if precipitating in seawater given coefficient partition defined from laboratory experiment (e.g., Hönisch et al., 2011). Barium sulphate BaSO₄ (barite) in pelagic environment is thought to precipitate via microbial activity (e.g., González-Munoz, 2003;Martinez-Ruiz et al., 2020) or through supersaturation of barium and sulphur in microenvironment that promotes precipitation abiotically (Dehairs, 1980;Bishop, 1988;Horner and Crockford, 2021 and references therein). Hence foraminifera calcifying in such a microenvironment would have their shell enriched in barium compared to the bulk seawater. Such a microenvironment could be a concern for paleo-pH

reconstructions as we expect variable pH alteration in marine aggregates. Marine aggregates dominated by algae can result in a pH increase if the signal is dominated by photosynthesis (e.g., Ploug et al., 1999) whilst aggregates dominated by organic matter degradation will release CO₂ and decrease pH by 0.22-0.91 (Alldredge and Cohen, 1987). Due to the technical challenges to collect intact marine aggregates from the water column and to measure pH with microelectrodes on sometimes floating aggregates, studies on pH alterations in marine aggregates are rare (Alldredge and Cohen, 1987) and further constraints are needed to quantify pH changes on multiple aggregates where *N. pachyderma* and *N. incompta* are observed to live.

540

545

555

560

565

570

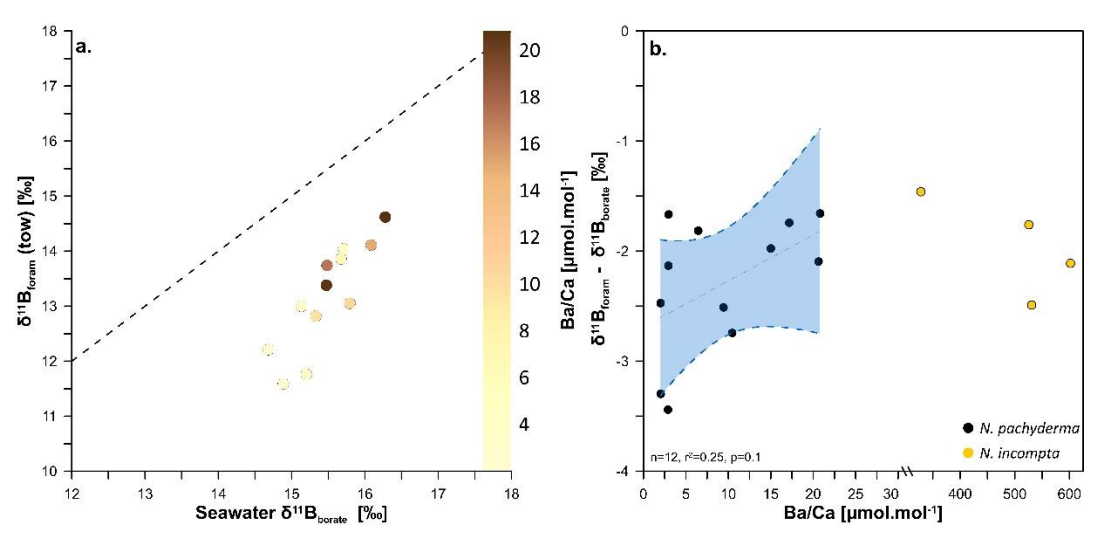


Figure 4. Relationship between the δ¹¹B of towed *N. pachyderma (coloured circles* with the δ¹¹B of seawater borate in relation to calcite Ba/Ca ratio. Panel a. shows δ¹¹B of towed specimens against δ¹¹B of seawater borate while the colour gradient is showing the respective Ba/Ca values. The 1:1 line is shown by the black dashed line. Panel b. is showing the regression between δ¹¹B_{foram}-δ¹¹B_{borate} offset of towed *N. pachyderma* specimens and Ba/Ca values (n=12, p=0.1, r2=0.25). The data are fitted with a linear regression (black line) and a 95% confidence envelope (blue shade). Also shown in panel b. are the high Ba/Ca values for *N. incompta* in yellow circles; please note the axis break.

If barium concentration is an accurate metric to trace this behaviour in N. pachyderma and N. incompta we would expect samples with high Ba/Ca to record a distinct pH and $\delta^{11}B$ from samples with low-Ba/Ca samples. Figure 4a shows some samples have higher barium than what is predicted by seawater following the partition coefficient $D_{Ba} = 0.11$ of other non-spinose foraminifera (Fehrenbacher et al., 2018), yet do not show any anomalous $\delta^{11}B$ compared to low-Ba/Ca samples. The elevated Ba/Ca results (> 30 umol/mol) need to be caveated by the fact that samples were not treated for barite removal during the cleaning process (as in Fehrenbacher et al., 2018), as this would lead to unacceptable sample loss for $\delta^{11}B$ measurement. The Ba/Ca ratio in N. incompta is distinct from N. pachyderma, with a range of 328-779 μmol/mol (vs. 1-21 μmol/mol for N. pachyderma). The species difference and trend of Ba/Ca values is observed in both tows and core tops. This striking contrast between the two species points towards a distinct behavioural difference between the two species, potentially suggesting N. incompta is more prone to live in marine aggregates or has a specific feeding behaviour that would favour Ba enrichment during calcification. The lack of any deviation in δ^{11} B space for these high-Ba samples (Figure 4b) suggest that the Ba enrichment observed did not result in a pH-altered microenvironment in marine aggregates influencing the δ^{11} B_{foram} and instead that Ba increase may be caused by other processes (e.g. feeding behaviour). In the absence of direct evidence of aggregate environment associated with high Ba/Ca for these two species, we conclude that the observed increase in Ba/Ca, either does not result in significant pH change or if it does, it does not compromise

the $\delta^{11}B$ proxy in the species examined here. The hypothesis that these species live in marine aggregate, and the link with Ba-enrichment requires further investigation through direct observation of intact marine aggregates in the water column (e.g. collected with a marine snow catcher) or newly formed in cultures, as well as direct measurement of pH change in the interstitial fluid of the aggregates and Ba/Ca in foraminifera shells.

4.3. δ^{11} B-derived CO₂ for core top values.

A comparison of available $\delta^{11}B_{foram}$ values measured on *N pachyderma* from previously published cores tops (Ezat et al., 2017;Henehan et al., 2016;Yu et al., 2013) with our tow-based calibration dataset shows that there is generally good agreement between *N. pachyderma* collected from tows and core tops (Figure 5). We note here that we recalculated seawater borate for the Yu et al. (2013) dataset using GLODAP v2 at 50 m instead of CARINA that was used in the original study. We used an anthropogenic DIC correction (C_{ANT}) on $\delta^{11}B_{borate}$ values for all core tops pre-dating the onset of anthropogenic CO₂ emissions (see Table S4 and S6), The core tops analysed in this study fall within the calibration uncertainties of the tow-based calibration equation except for Station 16. Further, the majority of the Yu et al. (2013) data falls below the calibration equation derived using the plankton tows.

There could be several reasons for the offsets between calibration studies. First, the estimated calcification depth of 50 m for these samples may be too shallow. A shift to a deeper depth habitat (e.g. 75-150 m) would reduce δ^{11} B_{borate} and thereby result in a better overall fit with the tow dataset (Figure S3). However, in the absence of stable isotopes we cannot constrain habitat depth with better accuracy. Further, the modern water column data including the correction factor for anthropogenic carbon to estimate seawater borate may not represent the actual calcification environment of *N pachyderma* preserved in core tops. For example, when the correction factor for anthropogenic carbon is removed for the Yu et al. (2013) dataset, the offset to the tow based calibration dataset is resolved. However, the pre-industrial ages for all but one core top in this dataset would strongly argue for the use of the correction factor for anthropogenic carbon. For station 16, it is possible that the sample from the multicore top 0-0.5 cm is modern or partially modern and should not be corrected for anthropogenic carbon. This is supported by the age model for gravity core M23411 (Baumann, 2007) collected at the same location as Station 16 providing Holocene sedimentation rates of 143 years per 0.5 cm. Therefore, the top 0-0.5 cm of sediments at this station could include a significant contribution of specimens grown after the onset of fossil fuel burning. However, in the absence of a date from the multicore top we cannot confirm it.

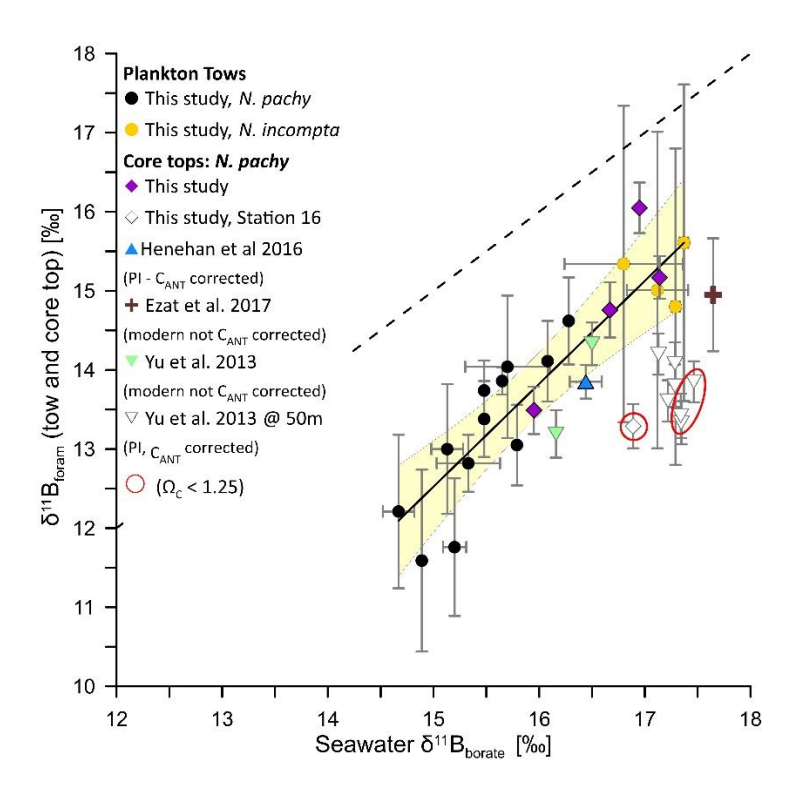


Figure 5. Compilation of plankton tows and core top δ¹¹B_{foram} versus δ¹¹B_{borate}. Here we plot our tow and core top results together with all available δ¹¹B_{foram} values measured on N. pachyderma (Henehan et al., 2016;Ezat et al., 2017;Yu et al., 2013). PI stands for preindustrial and C_{ANT} for anthropogenic carbon correction. The 1:1 line is shown by the black dashed line, and the solid black line shows the York regression of the tow dataset as shown in Figure 2 with the 95% confidence envelope (light yellow shade). The Yu et al., (2013) data is plotted with δ¹¹B_{borate} values estimated at 50 m. Please view Figure S3 for δ¹¹B_{borate} values estimated at 150 m.

Alternatively, the lower than expected δ¹¹B_{foram} values from the Yu et al. (2013) dataset may result from different size fractions used in the analysis. Here, core tops were sieved at a narrow size fraction of 200-250 μm, while Yu et al. (2013) used a larger range of 150–250 μm. Indeed, the offsets of *N. pachyderma* δ¹¹B_{foram} from δ¹¹B_{borate} are much larger for the Yu et al. (2013) dataset that includes smaller specimens. However, we note that our core tops are not offset from our plankton tow dataset which includes all size fractions. This would argue against a size effect. However, the apparent size effect could be reconciled if it is placed in the context of dissolution. For example, it has been observed that small foraminifera are more affected by dissolution than larger individuals as a result of their higher surface area to volume ratio (Berger and Piper, 1972;Berger et al., 1982). The cumulative effect of smaller size fractions and partial dissolution may therefore explain the apparent offset in the Yu et al. (2013) dataset (Ni et al., 2007).

620

625

Finally, δ^{11} B values recorded in crust calcite may be lower than in ontogenetic calcite. This has previously been suggested for *T. sacculifer*, where crust calcite is lower in δ^{11} B relative to ontogenetic calcite because symbionts are expelled or digested before gametogenic calcification begins (Ni et al., 2007). This loss of photosymbionts decreases the local pH due to the lack of photosynthetic activity and the δ^{11} B_{borate} of the microenvironment would be lower than ambient seawater values. Consequently, the crust calcite will be isotopically lighter than the ontogenetic calcite (Ni et al., 2007). However, *N. pachyderma* is asymbiotic and modern ecological observations would argue against a habitat migration to deeper depth during gametogenesis (Tell et al., 2022;Manno and Pavlov, 2014;Greco et al., 2019) and therefore it is unlikely that a difference in hydrographic conditions would

be responsible for a geochemical signature difference between ontogenetic and crust calcite. These ecological observations are supported by geochemical analysis of living (no crust) and dead (crust) *N. pachyderma* specimens collected from the same plankton nets (Hupp and Fehrenbacher, 2023), *N. incompta* and *N. dutertrei* specimen grown and crusted in culture under constant temperatures (Davis et al., 2017; WestgÅrd et al., 2023; Fehrenbacher et al., 2017) and *N. pachyderma* specimen from sediment traps (Jonkers et al., 2016).

630

655

660

665

635 The mechanisms responsible for the geochemical offsets observed in ontogenetic and crust calcite for N. pachyderma (e.g., Mg/Ca $\approx 15\%$ and δ^{18} O_c up to 2 ‰), remain unresolved, but are more likely linked to changes in the biomineralization process than hydrography. For example, faster calcification rates during the formation of crust calcite relative to the last whirl of chambers could result in variable kinetic fractionation during ontogeny and therefore variation in the degree of isotopically heavy B(OH)₃ incorporated into the foraminiferal calcite in 640 crusted specimen (Uchikawa et al., 2015; Farmer et al., 2019). If so, the degree of crusting would be an additional factor to consider when preparing specimens for analysis. Furthermore, the more soluble ontogenetic calcite (Wycech et al., 2018), could be prone to preferential dissolution (water column and sediments) relative to crust calcite, leaving core top N. pachyderma from sites close to undersaturation depleted in δ^{11} B values (Hönisch and Hemming, 2004; Ni et al., 2007; Seki et al., 2010). Indeed, we note that the low $\delta^{11}B$ values from Station 16 and 645 from some stations of the Yu et al. (2013) dataset have low bottom water $\Omega_C < 1.25$ values (Figure 4a, Table S5). Unfortunately, calcification rates are difficult to determine in culture for N. pachyderma as temperature control, especially at low temperatures, prevents prolonged periods of observations. Furthermore, there is no systematic δ^{11} B offset between crusted and uncrusted specimens preventing us at this stage from estimating a geochemical offset value between ontogenetic and crust calcite (e.g., Kozdon et al., 2009). Ongoing developments in $\delta^{11}B$ 650 single shell analysis vs MC-ICPMS laser ablation (Standish et al., 2019; Mayk et al., 2020; Raitzsch et al., 2020) N. pachyderma may provide enhanced spatial resolution to address the foraminifera test isotopic heterogeneity.

To assess whether the tow-based calibration can be used to estimate past pH and atmospheric CO_2 concentrations beyond these caveats we now treat the core tops as if they were an unknown paleo-sample. $\delta^{11}B$ derived CO_2 estimates from core tops in this study (except for station 16) provide CO_2 values that are consistent with atmospheric CO_2 observations made post 1900 (Figure 6). These results suggest that despite the low sedimentation rates; a proportion of modern foraminifera shells capture the anthropogenic CO_2 signal within the top 0-0.5 cm of surface sediments in the Nordic Seas. We also calculated atmospheric CO_2 using published core tops from Ezat et al. (2017) (which has larger uncertainties due to the additional uncertainties linked to differing analytical methods) and one core top from Yu et al. (2013) that we were able to pair with Mg/Ca values from the same multicore top published in Moffa-Sánchez et al. (2014). The highest reconstructed CO_2 values consistent with modern atmospheric CO_2 were measured in core tops that were confirmed modern by AMS ^{14}C dating (e.g., Station 12 and RAPID-35-25B). Applying the new calibration with a slope >1 to the downcore data of Yu et al. (2013), will elevate reconstructed surface seawater CO_2 . As a result, regions off Iceland in the polar North Atlantic may not have served as a sink of CO_2 to the atmosphere during the glacial and deglacial period as hypothesized in Yu et al. (2013). A detailed analysis of existing and new palaeoceanographic datasets will be the object of a forthcoming manuscript.

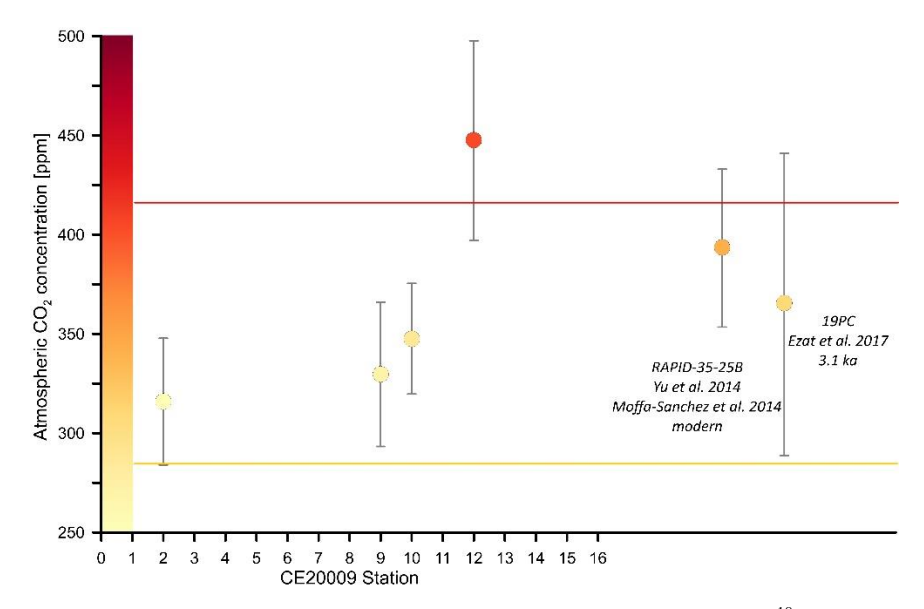


Figure 6. Atmospheric CO₂ concentration [ppm] derived using boron isotopes, Mg/Ca and δ¹⁸O_c from CE20009 core tops collected from the Nordic Seas (except station 16). Also shown are two core tops that have paired Mg/Ca and d18Oc values for *N. pachyderma* available. One from the Yu et al. (2013) dataset that we paired with Mg/Ca and δ¹⁸O_c from Moffa-Sánchez et al. (2014) and the other is from Ezat et al. (2017). The CO₂ uncertainty was calculated with a Monte Carlo simulation (see methods) See also Table S6.

5. Conclusion

680

685

Here we present the first tow-based open ocean $\delta^{11}B$ calibration of the non-spinose foraminifera *N. pachyderma* and *N. incompta* in the North Atlantic, complemented by core tops from similar locations. The use of tows allows us to precisely constrain the water chemistry in which foraminifera grew, bypassing the assumptions of foraminifera habitat depth and water chemistry typically encountered in core-top-based calibrations. We show that the signal recorded by these species is consistently below what is predicted by aqueous $\delta^{11}B_{\text{borate}}$, in line with other non-spinose foraminifera and that there is little evidence to support a strong influence of a temperature dependent α_B .

We propose instead that the lower-than-expected $\delta^{11}B_{\text{foram}}$ values are a result of active proton pumping during calcification raising the pH in the calcification fluid while the microenvironment surrounding the cell is undersaturated with respect to calcite as a result of respiration and calcification. The seemingly opposing signals can be reconciled when considering rapid boric acid diffusion between the calcifying fluid and the microenvironment around the foraminifera (Gagnon et al., 2021).

The addition of core top samples in the calibration does not significantly alter the slope of the calibration, giving confidence in the application of this tow-based calibration equation in downcore sediments. This is further supported when combining the δ¹¹B calibration with the Mg/Ca-δ¹⁸O correction scheme to reconstruct past atmospheric CO₂ concentrations. Given the rapid rise in recent atmospheric CO₂ concentrations, highly resolved marine archives when independently dated (e.g. ²¹⁰Pb), may be used to reconstruct ocean surface CO₂ and air-sea
 CO₂ fluxes over the past 200 years/the last glacial cycles and thereby provide crucial insight into ocean-atmosphere carbon fluxes since the onset of anthropogenic carbon emissions over deepwater formation regions. The application of the δ¹¹B calibration to recent marine archives may therefore allow us to answer critical open

questions about the role of the Nordic Seas as a carbon sink when deepwater formation was reduced (stronger) and sea ice extent was greater (reduced).

700

Data and materials availability

All data needed to evaluate the conclusions in the paper are presented in the paper and/or the Supplementary Materials.

705 Author contributions

E.D.L.V. carried out palaeoceanographic sample preparation and geochemical analysis of plankton tows and core tops from expedition CE20009, compiled and analysed all datasets, and wrote the original draft of the manuscript. A.M. conceptualized the project, acquired funding, carried out palaeoceanographic sample preparation of plankton tows from the Labrador Sea, coordinated the input of all co-authors and finalized the manuscript for publication. 710 M.R. performed trace element and boron isotope analysis on N. pachyderma plankton tow samples from the Labrador Sea. J.B. supervised A.M. at the Alfred Wegner Institute and oversaw trace element and boron isotope analysis. U.N. oversaw all stable isotope analyses of water and foraminifera samples from CE20009 and contributed to the final version of this manuscript. G.F. oversaw trace element and boron isotope analysis on N. pachyderma plankton tow samples from CE20009 and contributed to the final version of this manuscript. M.K. advised A.M. during project conceptualization, supervised her during her MSCA-IF at MARUM, University of 715 Bremen, and contributed to the final version of this manuscript. T.B. provided support to E.D.L.V. during boron isotope analysis and contributed to the final version of this manuscript. J.C.B. carried out palaeoceanographic sample preparation of plankton tows from expedition CE20009. M.E. provided sample material and contributed to the final version of this manuscript.

720

Competing interests

The contact author has declared that neither they nor their co-authors have any competing interests.

Funding Sources

This research was funded by MSCA-IF Project ARCTICO [838529] and the Marine Institute of Ireland Research Programme 2014-2020 (PDOC/19/05/02) awarded to AM. In addition, AM acknowledges the financial support of Science Foundation Ireland and the Geological Survey of Ireland under the SFI Frontiers for the Future Programme 21/FFP-P/10261 and Grant in Aid funding from the Marine Institute for research expedition CE20009 on the RV Celtic Explorer. M.R. acknowledges DFG (German Research Foundation) for funding through research grant no. RA 2068/4-1.

Acknowledgements

We gratefully acknowledge the support of the crew on the RV Celtic Explorer sailing under Master Anthony Hobin.

735 References

- Alldredge, A. L., and Cohen, Y.: Can microscale chemical patches persist in the sea? Microelectrode study of marine snow, fecal pellets, Science, 235, 689-691, 1987.
- Altuna, N. E. B., Pieńkowski, A. J., Eynaud, F., and Thiessen, R.: The morphotypes of Neogloboquadrina pachyderma: Isotopic signature and distribution patterns in the Canadian Arctic Archipelago and adjacent regions, Marine Micropaleontology, 142, 13-24, 2018.
- Anagnostou, E., Huang, K.-F., You, C.-F., Sikes, E., and Sherrell, R.: Evaluation of boron isotope ratio as a pH proxy in the deep sea coral Desmophyllum dianthus: Evidence of physiological pH adjustment, Earth and Planetary Science Letters, 349, 251-260, 2012.
- Anagnostou, E., Williams, B., Westfield, I., Foster, G., and Ries, J.: Calibration of the pH-δ11B and temperature-Mg/Li proxies in the long-lived high-latitude crustose coralline red alga Clathromorphum compactum via controlled laboratory experiments, Geochimica et Cosmochimica Acta, 254, 142-155, 2019.
 - Anand, P., Elderfield, H., and Conte, M. H.: Calibration of Mg/Ca thermometry in planktonic foraminifera from a sediment trap time series, Paleoceanography, 18, 1050, 10.1029/2002pa000846, 2003.
- Azetsu-Scott, K., Clarke, A., Falkner, K., Hamilton, J., Jones, E. P., Lee, C., Petrie, B., Prinsenberg, S., Starr,
 M., and Yeats, P.: Calcium carbonate saturation states in the waters of the Canadian Arctic Archipelago and the Labrador Sea, Journal of Geophysical Research: Oceans, 115, 2010.
 - Barker, S., Greaves, M., and Elderfield, H.: A study of cleaning procedures used for foraminiferal Mg/Ca paleothermometry, Geochemistry Geophysics Geosystems, 4, 8407, doi:10.1029/2003GC000559, 2003.
- Bauch, D., Carstens, J., and Wefer, G.: Oxygen isotope composition of living Neogloboquadrina pachyderma 755 (sin.) in the Arctic Ocean, Earth and Planetary Science Letters, 146, 47-58, 1997.
 - Baumann, A.: Dinoflagellaten-Zysten als Paläoumweltindikatoren im Spätquartär des Europäischen Nordmeeres, Universität Bremen, 2007.
 - Bentov, S., Brownlee, C., and Erez, J.: The role of seawater endocytosis in the biomineralization process in calcareous foraminifera, Proceedings of the National Academy of Sciences, 106, 21500-21504, 2009.
- 760 Bereiter, B., Eggleston, S., Schmitt, J., Nehrbass-Ahles, C., Stocker, T. F., Fischer, H., Kipfstuhl, S., and Chappellaz, J.: Revision of the EPICA Dome C CO2 record from 800 to 600 kyr before present, Geophysical Research Letters, 42, 542-549, 2015.
 - Berger, W. H., and Piper, D. J. W.: Planktonic foraminifera: differential settling, dissolution, and redeposition, Limnology Oceanography, 17, 275-287, 1972.
- Herger, W. H., Bonneau, M.-C., and Parker, F. L.: Foraminifera on the deep-sea floor: lysocline and dissolution rate, Oceanologica Acta, 5, 249-258, 1982.

- Bishop, J. K.: The barite-opal-organic carbon association in oceanic particulate matter., Nature, no. 6162, 341-343, 1988.
- Burke, J. E., Renema, W., Schiebel, R., and Hull, P. M.: Three-dimensional analysis of inter-and intraspecific variation in ontogenetic growth trajectories of planktonic foraminifera, Marine Micropaleontology, 155, 101794, 2020.
 - Chalk, T. B., Hain, M. P., Foster, G. L., Rohling, E. J., Sexton, P. F., Badger, M. P., Cherry, S. G., Hasenfratz, A. P., Haug, G. H., and Jaccard, S. L.: Causes of ice age intensification across the Mid-Pleistocene Transition, Proceedings of the National Academy of Sciences, 114, 13114-13119, 2017.
- 775 Cifelli, R.: Globigerina incompta, a new species of pelagic foraminifera from the North Atlantic, Contributions from the Cushman Foundation for Foraminiferal Research, 12, 83-86, 1961.
 - Consortium, C. C. P. I. P., Hönisch, B., Royer, D. L., Breecker, D. O., Polissar, P. J., Bowen, G. J., Henehan, M. J., Cui, Y., Steinthorsdottir, M., and McElwain, J. C.: Toward a Cenozoic history of atmospheric CO2, Science, 382, eadi5177, 2023.
- Darling, K. F., Kucera, M., Kroon, D., and Wade, C. M.: A resolution for the coiling direction paradox in Neogloboquadrina pachyderma, Paleoceanography, 21, 2006.
 - Davis, C. V., Fehrenbacher, J. S., Hill, T. M., Russell, A. D., and Spero, H. J.: Relationships Between Temperature, pH, and Crusting on Mg/Ca Ratios in Laboratory-Grown Neogloboquadrina Foraminifera, Paleoceanography, 32, 1137-1152, 2017.
- Davis, C. V., Livsey, C. M., Palmer, H. M., Hull, P. M., Thomas, E., Hill, T. M., and Benitez-Nelson, C. R.: Extensive morphological variability in asexually produced planktic foraminifera, Science Advances, 6, eabb8930, 2020.
- de la Vega, E., Chalk, T. B., Hain, M. P., Wilding, M. R., Casey, D., Gledhill, R., Luo, C., Wilson, P. A., and Foster, G. L.: Orbital CO 2 reconstruction using boron isotopes during the late Pleistocene, an assessment of accuracy, Climate of the Past Discussions, 2023, 1-26, 2023.
 - de Nooijer, L. d., Spero, H., Erez, J., Bijma, J., and Reichart, G.-J.: Biomineralization in perforate foraminifera, Earth-Science Reviews, 135, 48-58, 2014.
 - de Nooijer, L. J., Toyofuku, T., and Kitazato, H.: Foraminifera promote calcification by elevating their intracellular pH, Proceedings of the National Academy of Sciences, 106, 15374-15378, 2009.
- Dehairs, F., Chesselet, R. and Jedwab, J.: Discrete suspended particles of barite and the barium cycle in the open ocean, Earth and Planetary Science Letters, 49(2), 528-550, https://doi.org/10.1016/0012-821X(80)90094-1, 1980.

- Dekens, P. S., Lea, D. W., Pak, D. K., and Spero, H. J.: Core top calibration of Mg/Ca in tropical foraminifera: Refining paleotemperature estimation, Geochemistry Geophysics Geosystems, 3, 1022, 10.1029/2001gc000200, 2002.
 - Dickson, A.: Thermodynamics of the dissociation of boric acid in synthetic seawater from 273.15 to 318.15 K, Deep Sea Research Part A. Oceanographic Research Papers, 37, 755-766, 1990.
 - Erez, J., and Honjo, S.: Comparison of isotopic composition of planktonic foraminifera in plankton tows, sediment traps and sediments, Palaeogeogr. Palaeoclimatol. Palaeocol., 33, 129-156, 1981.
- 805 Evans, D., Müller, W., and Erez, J.: Assessing foraminifera biomineralisation models through trace element data of cultures under variable seawater chemistry, Geochimica et Cosmochimica Acta, 236, 198-217, 2018.
 - Ezat, M. M., Rasmussen, T. L., Hönisch, B., Groeneveld, J., and Demenocal, P.: Episodic release of CO2 from the high-latitude North Atlantic Ocean during the last 135 kyr, Nature Communications, 8, 14498, 2017.
- Farmer, J. R., Hönisch, B., and Uchikawa, J.: Single laboratory comparison of MC-ICP-MS and N-TIMS boron isotope analyses in marine carbonates, Chemical Geology, 447, 173-182, 2016.
 - Farmer, J. R., Branson, O., Uchikawa, J., Penman, D. E., Hönisch, B., and Zeebe, R. E.: Boric acid and borate incorporation in inorganic calcite inferred from B/Ca, boron isotopes and surface kinetic modeling, Geochimica et Cosmochimica Acta, 244, 229-247, 2019.
- Fehrenbacher, J. S., Russell, A. D., Davis, C. V., Gagnon, A. C., Spero, H. J., Cliff, J. B., Zhu, Z., and Martin,
 P.: Link between light-triggered Mg-banding and chamber formation in the planktic foraminifera
 Neogloboquadrina dutertrei, Nature Communications, 8, 15441, 2017.
 - Fehrenbacher, J. S., Russell, A. D., Davis, C. V., Spero, H. J., Chu, E., and Hönisch, B.: Ba/Ca ratios in the non-spinose planktic foraminifer Neogloboquadrina dutertrei: Evidence for an organic aggregate microhabitat, Geochimica et Cosmochimica Acta, 236, 361-372, 2018.
- Foster, G.: Seawater pH, pCO 2 and [CO 2–3] variations in the Caribbean Sea over the last 130 kyr: a boron isotope and B/Ca study of planktic foraminifera, Earth and Planetary Science Letters, 271, 254-266, 2008.
 - Foster, G., Pogge von Strandmann, P. A., and Rae, J.: Boron and magnesium isotopic composition of seawater, Geochemistry, Geophysics, Geosystems, 11, 2010.
- Foster, G. L., Hönisch, B., Paris, G., Dwyer, G. S., Rae, J. W., Elliott, T., Gaillardet, J., Hemming, N. G.,
 Louvat, P., and Vengosh, A.: Interlaboratory comparison of boron isotope analyses of boric acid, seawater and
 marine CaCO3 by MC-ICPMS and NTIMS, Chemical Geology, 358, 1-14, 2013.
 - Foster, G. L., and Rae, J. W.: Reconstructing ocean pH with boron isotopes in foraminifera, Annual Review of Earth and Planetary Sciences, 44, 207-237, 2016.

- Fritz-Endres, T., Fehrenbacher, J. S., Russell, A. D., and Cynar, H.: Increased productivity in the equatorial pacific during the deglaciation inferred from the Ba/Ca ratios of non-spinose planktic foraminifera, Paleoceanography and Paleoclimatology, 37, e2022PA004506, 2022.
 - Gagnon, A. C., Gothmann, A. M., Branson, O., Rae, J. W., and Stewart, J. A.: Controls on boron isotopes in a cold-water coral and the cost of resilience to ocean acidification, Earth and Planetary Science Letters, 554, 116662, 2021.
- 635 Gaillardet, J., Lemarchand, D., Göpel, C., and Manhès, G.: Evaporation and sublimation of boric acid: application for boron purification from organic rich solutions, Geostandards Newsletter, 25, 67-75, 2001.
 - Gilbert, P. U., Bergmann, K. D., Boekelheide, N., Tambutté, S., Mass, T., Marin, F., Adkins, J. F., Erez, J., Gilbert, B., and Knutson, V.: Biomineralization: Integrating mechanism and evolutionary history, Science advances, 8, eabl9653, 2022.
- 600 González-Munoz, M. T., Belén Fernández-Luque, Francisca Martínez-Ruiz, Kaoutar Ben Chekroun, José María Arias, Manuel Rodríguez-Gallego, Magdalena Martínez-Canamero, Concepción de Linares, and Adina Paytan: Precipitation of barite by Myxococcus xanthus: possible implications for the biogeochemical cycle of barium, Applied and Environmental Microbiology, 69.9, https://doi.org/10.1128/AEM.69.9.5722-5725.2003, 2003.
- Gray, W. R., and Evans, D.: Nonthermal influences on Mg/Ca in planktonic foraminifera: A review of culture studies and application to the last glacial maximum, Paleoceanography and Paleoclimatology, 34, 306-315, 2019.
 - Greco, M., Jonkers, L., Kretschmer, K., Bijma, J., and Kucera, M.: Depth habitat of the planktonic foraminifera < i> Neogloboquadrina pachyderma </i> in the northern high latitudes explained by sea-ice and chlorophyll concentrations, Biogeosciences, 16, 3425-3437, 2019.
- Guillermic, M., Misra, S., Eagle, R., Villa, A., Chang, F., and Tripati, A.: Seawater pH reconstruction using boron isotopes in multiple planktonic foraminifera species with different depth habitats and their potential to constrain pH and pCO2 gradients, Biogeosciences, 17, 3487-3510, 10.5194/bg-17-3487-2020, 2020.
- Gutjahr, M., Bordier, L., Douville, E., Farmer, J., Foster, G. L., Hathorne, E. C., Hönisch, B., Lemarchand, D., Louvat, P., and McCulloch, M.: Sub-permil interlaboratory consistency for solution-based boron isotope analyses on marine carbonates, Geostandards and Geoanalytical Research, 45, 59-75, 2021.
 - Hansen, B., and Østerhus, S.: North atlantic-nordic seas exchanges, Progress in oceanography, 45, 109-208, 2000.
- Hathorne, E. C., Gagnon, A., Felis, T., Adkins, J., Asami, R., Boer, W., Caillon, N., Case, D., Cobb, K. M., and Douville, E.: Interlaboratory study for coral Sr/Ca and other element/Ca ratio measurements, Geochemistry,
 Geophysics, Geosystems, 14, 3730-3750, 2013.

- Henehan, M. J., Rae, J. W., Foster, G. L., Erez, J., Prentice, K. C., Kucera, M., Bostock, H. C., Martínez-Botí, M. A., Milton, J. A., and Wilson, P. A.: Calibration of the boron isotope proxy in the planktonic foraminifera Globigerinoides ruber for use in palaeo-CO2 reconstruction, Earth and Planetary Science Letters, 364, 111-122, 2013.
- Henehan, M. J., Foster, G. L., Rae, J. W., Prentice, K. C., Erez, J., Bostock, H. C., Marshall, B. J., and Wilson,
 P. A.: Evaluating the utility of B/Ca ratios in planktic foraminifera as a proxy for the carbonate system: A case study of Globigerinoides ruber, Geochemistry, Geophysics, Geosystems, 16, 1052-1069, 2015.
 - Henehan, M. J., Foster, G. L., Bostock, H. C., Greenop, R., Marshall, B. J., and Wilson, P. A.: A new boron isotope-pH calibration for Orbulina universa, with implications for understanding and accounting for 'vital effects', Earth and Planetary Science Letters, 454, 282-292, 2016.
 - Hönisch, B., Bijma, J., Russell, A. D., Spero, H. J., Palmer, M. R., Zeebe, R. E., and Eisenhauer, A.: The influence of symbiont photosynthesis on the boron isotopic composition of foraminifera shells, Marine Micropaleontology, 49, 87-96, 2003.
- Hönisch, B., and Hemming, N. G.: Ground-truthing the boron isotope-paleo-pH proxy in planktonic foraminifera shells: Partial dissolution and shell size effects, Paleoceanography, 19, 2004.

870

885

- Hönisch, B., Allen, K. A., Russell, A. D., Eggins, S. M., Bijma, J., Spero, H. J., Lea, D. W., and Yu, J.: Planktic foraminifers as recorders of seawater Ba/Ca, Marine Micropaleontology, 79, 52-57, https://doi.org/10.1016/j.marmicro.2011.01.003, 2011.
- Hönisch, B., Eggins, S. M., Haynes, L. L., Allen, K. A., Holland, K. D., and Lorbacher, K.: Boron proxies in paleoceanography and paleoclimatology, 2019.
 - Horner, T. J., and Crockford, P. W.: Barium isotopes: Drivers, dependencies, and distributions through space and time, Cambridge University Press, 2021.
 - Hupp, B. N., and Fehrenbacher, J. S.: Geochemical differences between alive, uncrusted and dead, crusted shells of Neogloboquadrina pachyderma: Implications for paleoreconstruction, Paleoceanography and Paleoclimatology, 38, e2023PA004638, 2023.
 - Johnson, G. C.: Quantifying Antarctic bottom water and North Atlantic deep water volumes, Journal of Geophysical Research: Oceans, 113, 2008.
- Jonkers, L., Brummer, G. J. A., Peeters, F. J., van Aken, H. M., and De Jong, M. F.: Seasonal stratification, shell flux, and oxygen isotope dynamics of left-coiling N. pachyderma and T. quinqueloba in the western subpolar North Atlantic, Paleoceanography, 25, 2010.
 - Jonkers, L., Heuven, S., Zahn, R., and Peeters, F. J.: Seasonal patterns of shell flux, δ18O and δ13C of small and large N. pachyderma (s) and G. bulloides in the subpolar North Atlantic, Paleoceanography, 28, 164-174, 2013.

Jonkers, L., Buse, B., Brummer, G.-J. A., and Hall, I. R.: Chamber formation leads to Mg/Ca banding in the planktonic foraminifer Neogloboquadrina pachyderma, Earth and Planetary Science Letters, 451, 177-184, 2016.

895

- Jonkers, L., Brummer, G.-J. A., Meilland, J., Groeneveld, J., and Kucera, M.: Variability in Neogloboquadrina pachyderma stable isotope ratios from isothermal conditions: implications for individual foraminifera analysis, Climate of the Past, 18, 89-101, 2022.
- King, A. L., and Howard, W. R.: δ18O seasonality of planktonic foraminifera from Southern Ocean sediment
 traps: Latitudinal gradients and implications for paleoclimate reconstructions, Marine Micropaleontology, 56, 1-24, 2005.
 - Klochko, K., Kaufman, A. J., Yao, W., Byrne, R. H., and Tossell, J. A.: Experimental measurement of boron isotope fractionation in seawater, Earth and Planetary Science Letters, 248, 276-285, 2006.
- Kohfeld, K. E., Fairbanks, R. G., Smith, S. L., and Walsh, I. D.: Neogloboquadrina pachyderma (sinistral coiling) as paleoceanographic tracers in polar oceans: Evidence from Northeast Water Polynya plankton tows, sediment traps, and surface sediments, Paleoceanography, 11, 679-699, 1996.
 - Kozdon, R., Ushikubo, T., Kita, N., Spicuzza, M., and Valley, J.: Intratest oxygen isotope variability in the planktonic foraminifer N. pachyderma: Real vs. apparent vital effects by ion microprobe, Chemical Geology, 258, 327-337, 2009.
- 910 Lauvset, S. K., Lange, N., Tanhua, T., Bittig, H. C., Olsen, A., Kozyr, A., Alin, S. R., Álvarez, M., Azetsu-Scott, K., and Barbero, L.: GLODAPv2. 2022: the latest version of the global interior ocean biogeochemical data product, Earth System Science Data Discussions, 2022, 1-37, 2022.
 - Lea, D., Mashiotta, T. A., and Spero, H. J.: Controls on magnesium and strontium uptake in planktonic foraminifera determined by live culturing, Geochimica et Cosmochimica Acta, 63, 2369-2379, 1999.
- 915 Lee, K., Kim, T.-W., Byrne, R. H., Millero, F. J., Feely, R. A., and Liu, Y.-M.: The universal ratio of boron to chlorinity for the North Pacific and North Atlantic oceans, Geochimica et Cosmochimica Acta, 74, 1801-1811, 2010.
- Livsey, C. M., Kozdon, R., Bauch, D., Brummer, G. J. A., Jonkers, L., Orland, I., Hill, T. M., and Spero, H. J.: High-resolution Mg/Ca and δ18O patterns in modern Neogloboquadrina pachyderma from the Fram Strait and
 Irminger Sea, Paleoceanography and Paleoclimatology, 35, e2020PA003969, 2020.
 - Lombard, F., Labeyrie, L., Michel, E., Bopp, L., Cortijo, E., Retailleau, S., Howa, H., and Jorissen, F.: Modelling planktic foraminifer growth and distribution using an ecophysiological multi-species approach, Biogeosciences, 8, 853, 2011.
- Manno, C., and Pavlov, A.: Living planktonic foraminifera in the Fram Strait (Arctic): absence of diel vertical migration during the midnight sun, Hydrobiologia, 721, 285-295, 2014.

- Martínez-Botí, M., Mortyn, P., Schmidt, D., Vance, D., and Field, D.: Mg/Ca in foraminifera from plankton tows: Evaluation of proxy controls and comparison with core tops, Earth and Planetary Science Letters, 307, 113-125, 2011.
- Martínez-Botí, M. A., Marino, G., Foster, G. L., Ziveri, P., Henehan, M. J., Rae, J. W., Mortyn, P. G., and Vance, D.: Boron isotope evidence for oceanic carbon dioxide leakage during the last deglaciation, Nature, 518, 219, 2015.
 - Martinez-Ruiz, F., Paytan, A., Gonzalez-Munoz, M., Jroundi, F., Abad, M. d. M., Lam, P. J., Horner, T. J., and Kastner, M.: Barite precipitation on suspended organic matter in the mesopelagic zone, Frontiers in Earth Science, 8, 567714, 2020.
- 935 Mayk, D., Fietzke, J., Anagnostou, E., and Paytan, A.: LA-MC-ICP-MS study of boron isotopes in individual planktonic foraminifera: A novel approach to obtain seasonal variability patterns, Chemical Geology, 531, 119351, 2020.
- McCulloch, M., Trotter, J., Montagna, P., Falter, J., Dunbar, R., Freiwald, A., Försterra, G., Correa, M. L., Maier, C., and Rüggeberg, A.: Resilience of cold-water scleractinian corals to ocean acidification: Boron isotopic systematics of pH and saturation state up-regulation, Geochimica et Cosmochimica Acta, 87, 21-34, 2012.
 - Meilland, J., Siccha, M., Kaffenberger, M., Bijma, J., and Kucera, M.: Population dynamics and reproduction strategies of planktonic foraminifera in the open ocean, Biogeosciences, 18, 5789-5809, 2021.
- Mikis, A., Hendry, K. R., Pike, J., Schmidt, D. N., Edgar, K. M., Peck, V., Peeters, F. J., Leng, M. J., Meredith,
 M. P., and Jones, C. L.: Temporal variability in foraminiferal morphology and geochemistry at the West Antarctic Peninsula: a sediment trap study, Biogeosciences, 16, 3267-3282, 2019.
 - Misra, S., Owen, R., Kerr, J., Greaves, M., and Elderfield, H.: Determination of $\delta 11B$ by HR-ICP-MS from mass limited samples: Application to natural carbonates and water samples, Geochimica et Cosmochimica Acta, 140, 531-552, 2014.
- Moffa-Sánchez, P., Hall, I. R., Barker, S., Thornalley, D. J., and Yashayaev, I.: Surface changes in the eastern Labrador Sea around the onset of the Little Ice Age, Paleoceanography, 29, 160-175, 2014.
 - Morley, A., de la Vega, E., Raitzsch, M., Bijma, J., Ninnemann, U., Foster, G., Chalk, T. B., Meilland, J., Cave, R., and Büscher, J.: A solution for constraining past marine Polar Amplification, Nature Communications, 15, 9002, 2024.
- 955 Mortyn, P. G., and Charles, C. D.: Planktonic foraminiferal depth habitat and δ18O calibrations: Plankton tow results from the Atlantic sector of the Southern Ocean, Paleoceanography, 18, 2003.

- Ni, Y., Foster, G. L., Bailey, T., Elliott, T., Schmidt, D. N., Pearson, P., Haley, B., and Coath, C.: A core top assessment of proxies for the ocean carbonate system in surface-dwelling foraminifers, Paleoceanography, 22, 2007.
- Nickoloff, G., Else, B., Ahmed, M., Burgers, T., Miller, L., and Papakyriakou, T.: Strong pCO2 undersaturation in an Arctic sea: A decade of spatial and temporal variability in Baffin Bay, Journal of Geophysical Research: Oceans, 129, e2023JC020595, 2024.
- Østerhus, S., Woodgate, R., Valdimarsson, H., Turrell, B., De Steur, L., Quadfasel, D., Olsen, S. M., Moritz,
 M., Lee, C. M., and Larsen, K. M. H.: Arctic Mediterranean exchanges: a consistent volume budget and trends
 in transports from two decades of observations, Ocean Science, 15, 379-399, 2019.
 - Pados, T., and Spielhagen, R. F.: Species distribution and depth habitat of recent planktic foraminifera in Fram Strait, Arctic Ocean, Polar Research, 33, 22483, 2014.
 - Ploug, H., Grossart, H.-P., Azam, F., and Jorgensen, B. B.: Photosynthesis, respiration, and carbon turnover in sinking marine snow from surface waters of Southern California Bight: implications for the carbon cycle,
- 970 Marine Ecology Progress Series, 179, 1-11, 1999.
 - Rae, J. W., Foster, G. L., Schmidt, D. N., and Elliott, T.: Boron isotopes and B/Ca in benthic foraminifera: Proxies for the deep ocean carbonate system, Earth and Planetary Science Letters, 302, 403-413, 2011.
- Raitzsch, M., Bijma, J., Benthien, A., Richter, K.-U., Steinhoefel, G., and Kučera, M.: Boron isotope-based seasonal paleo-pH reconstruction for the Southeast Atlantic–A multispecies approach using habitat preference of planktonic foraminifera, Earth and Planetary Science Letters, 487, 138-150, 2018.
 - Raitzsch, M., Rollion-Bard, C., Horn, I., Steinhoefel, G., Benthien, A., Richter, K.-U., Buisson, M., Louvat, P., and Bijma, J.: Single-shell δ 11 B analysis of Cibicidoides wuellerstorfi using femtosecond laser ablation MC-ICPMS and secondary ion mass spectrometry, Biogeosciences, 17, 5365-5375, 2020.
- Ravelo, A. C., and Hillaire-Marcel, C.: Chapter eighteen the use of oxygen and carbon isotopes of foraminifera in paleoceanography, Developments in marine geology, 1, 735-764, 2007.
 - Raven, J. A., and Falkowski, P. G.: Oceanic sinks for atmospheric CO2, Plant, Cell & Environment, 22, 741-755, 1999.
- Richey, J. N., Fehrenbacher, J. S., Reynolds, C. E., Davis, C. V., and Spero, H. J.: Barium enrichment in the non-spinose planktic foraminifer, Globorotalia truncatulinoides, Geochimica et Cosmochimica Acta, 333, 184 199, 2022.
 - Rink, S., Kühl, M., Bijma, J., and Spero, H.: Microsensor studies of photosynthesis and respiration in the symbiotic foraminifer Orbulina universa, Marine Biology, 131, 583-595, 1998.

- Rysgaard, S., Bendtsen, J., Pedersen, L. T., Ramløv, H., and Glud, R. N.: Increased CO2 uptake due to sea ice growth and decay in the Nordic Seas, Journal of Geophysical Research: Oceans, 114, 2009.
- 990 Sanyal, A., Bijma, J., Spero, H., and Lea, D. W.: Empirical relationship between pH and the boron isotopic composition of Globigerinoides sacculifer: Implications for the boron isotope paleo-pH proxy, Paleoceanography, 16, 515-519, 2001.
 - Schlitzer, R.: Interactive analysis and visualization of geoscience data with Ocean Data View, Computers & Geosciences, 28, 1211-1218, https://doi.org/10.1016/S0098-3004(02)00040-7, 2002.
- 995 Schmittner, A., and Galbraith, E. D.: Glacial greenhouse-gas fluctuations controlled by ocean circulation changes, Nature, 456, 373-376, 2008.
 - Seki, O., Foster, G. L., Schmidt, D. N., Mackensen, A., Kawamura, K., and Pancost, R. D.: Alkenone and boron-based Pliocene pCO2 records, Earth and Planetary Science Letters, 292, 201-211, 2010.
- Shackleton, N.: Attainment of isotopic equilibrium between ocean water and the benthonic foraminifera genus *Uvigerina*: Isotopic changes in the ocean during the last glacial, Colloq. Int. C.N.R.S., 219, 203-209, 1974.
 - Shuttleworth, R., Bostock, H., Chalk, T. B., Calvo, E., Jaccard, S., Pelejero, C., Martínez-García, A., and Foster, G.: Early deglacial CO2 release from the Sub-Antarctic Atlantic and Pacific oceans, Earth and Planetary Science Letters, 554, 116649, 2021.
- Si, W., Novak, J. B., Richter, N., Polissar, P., Ma, R., Santos, E., Nirenberg, J., Herbert, T. D., and Aubry, M.-1005 P.: Alkenone-derived estimates of Cretaceous p CO2, Geology, 52, 555-559, 2024.
 - Simstich, J., Sarnthein, M., and Erlenkeuser, H.: Paired δ 18 O signals of Neogloboquadrina pachyderma (s) and Turborotalita quinqueloba show thermal stratification structure in Nordic Seas, Marine Micropaleontology, 48, 107-125, 2003.
- Standish, C. D., Chalk, T. B., Babila, T. L., Milton, J. A., Palmer, M. R., and Foster, G. L.: The effect of matrix interferences on in situ boron isotope analysis by laser ablation multi-collector inductively coupled plasma mass spectrometry, Rapid Communications in Mass Spectrometry, 33, 959-968, 2019.
 - Stangeew, E.: Distribution and Isotopic Composition of Living Planktonic Foraminifera N. pachyderma (sinistral) and T. quinqueloba in the High Latitude North Atlantic, Christian-Albrechts Universität Kiel, 2001.
- Stewart, J. A., Anagnostou, E., and Foster, G. L.: An improved boron isotope pH proxy calibration for the deepsea coral Desmophyllum dianthus through sub-sampling of fibrous aragonite, Chemical Geology, 447, 148-160, 2016.
 - Stewart, J. A., Christopher, S. J., Kucklick, J. R., Bordier, L., Chalk, T. B., Dapoigny, A., Douville, E., Foster, G. L., Gray, W. R., and Greenop, R.: NIST RM 8301 boron isotopes in marine carbonate (simulated coral and

- foraminifera solutions): Inter-laboratory δ11B and trace element ratio value assignment, Geostandards and 1020 Geoanalytical Research, 45, 77-96, 2021.
 - Sulpis, O., Lauvset, S. K., and Hagens, M.: Current estimates of K 1* and K 2* appear inconsistent with measured CO 2 system parameters in cold oceanic regions, Ocean Science Discussions, 2020, 1-27, 2020.
- Takahashi, T., Sutherland, S. C., Wanninkhof, R., Sweeney, C., Feely, R. A., Chipman, D. W., Hales, B., Friederich, G., Chavez, F., and Sabine, C.: Climatological mean and decadal change in surface ocean pCO2, and net sea–air CO2 flux over the global oceans, Deep Sea Research Part II: Topical Studies in Oceanography, 56, 554-577, 2009.
 - Takahashi, T., Sutherland, S. C., and Kozyr, A.: Global ocean surface water partial pressure of CO2 database: Measurements performed during 1957–2018 (version 2018), NOAA/NCEI/OCADS NDP-088 (V2018) Rep., 25 pp., https://www.ncei.noaa.gov..., 2019.
- Tell, F., Jonkers, L., Meilland, J., and Kucera, M.: Upper-ocean flux of biogenic calcite produced by the Arctic planktonic foraminifera Neogloboquadrina pachyderma, Biogeosciences, 19, 4903-4927, 2022.
 - Toyofuku, T., Matsuo, M. Y., De Nooijer, L. J., Nagai, Y., Kawada, S., Fujita, K., Reichart, G.-J., Nomaki, H., Tsuchiya, M., and Sakaguchi, H.: Proton pumping accompanies calcification in foraminifera, Nature Communications, 8, 14145, 2017.
- 1035 Uchikawa, J., Penman, D. E., Zachos, J. C., and Zeebe, R. E.: Experimental evidence for kinetic effects on B/Ca in synthetic calcite: implications for potential B (OH) 4– and B (OH) 3 incorporation, Geochimica et Cosmochimica Acta, 150, 171-191, 2015.
 - Ujiié, Y., Ishitani, Y., Nagai, Y., Takaki, Y., Toyofuku, T., and Ishii, S. i.: Unique evolution of foraminiferal calcification to survive global changes, Science Advances, 9, eadd3584, 2023.
- 1040 Volkmann, R., and Mensch, M.: Stable isotope composition (δ18O, δ13C) of living planktic foraminifers in the outer Laptev Sea and the Fram Strait, Marine Micropaleontology, 42, 163-188, 2001.
 - Wang, B.-S., You, C.-F., Huang, K.-F., Wu, S.-F., Aggarwal, S. K., Chung, C.-H., and Lin, P.-Y.: Direct separation of boron from Na-and Ca-rich matrices by sublimation for stable isotope measurement by MC-ICP-MS, Talanta, 82, 1378-1384, 2010.
- Weiss, R. F.: Carbon dioxide in water and seawater: The solubility of a non-ideal gas, Marine Chemistry, 2, 203-215, 1974.
 - WestgÅrd, A., Ezat, M. M., Chalk, T. B., Chierici, M., Foster, G. L., and Meilland, J.: Large-scale culturing of Neogloboquadrina pachyderma, its growth in, and tolerance of, variable environmental conditions, Journal of Plankton Research, 45, 732-745, 2023.

- Winkelbauer, H. A., Hoogakker, B. A., Chance, R. J., Davis, C. V., Anthony, C. J., Bischoff, J., Carpenter, L. J., Chenery, S. R., Hamilton, E. M., and Holdship, P.: Planktic foraminifera iodine/calcium ratios from plankton tows, Frontiers in Marine Science, 10, 1095570, 2023.
- Wycech, J. B., Kelly, D. C., Kitajima, K., Kozdon, R., Orland, I. J., and Valley, J. W.: Combined effects of gametogenic calcification and dissolution on δ18O measurements of the planktic foraminifer Trilobatus
 sacculifer, Geochemistry, Geophysics, Geosystems, 19, 4487-4501, 2018.
 - Yasunaka, S., Manizza, M., Terhaar, J., Olsen, A., Yamaguchi, R., Landschützer, P., Watanabe, E., Carroll, D., Adiwira, H., and Müller, J. D.: An assessment of CO2 uptake in the Arctic Ocean from 1985 to 2018, Global Biogeochemical Cycles, 37, e2023GB007806, 2023.
- York, D., Evensen, N. M., Martínez, M. L., and De Basabe Delgado, J.: Unified equations for the slope, intercept, and standard errors of the best straight line, American journal of physics, 72, 367-375, 2004.
 - Yu, J., Thornalley, D. J., Rae, J. W., and McCave, N. I.: Calibration and application of B/Ca, Cd/Ca, and δ11B in Neogloboquadrina pachyderma (sinistral) to constrain CO2 uptake in the subpolar North Atlantic during the last deglaciation, Paleoceanography, 28, 237-252, 2013.
- Zeebe, R. E., Bijma, J., and Wolf-Gladrow, D. A.: A diffusion-reaction model of carbon isotope fractionation in foraminifera, Marine Chemistry, 64, 199-127, 1999.
 - Zeebe, R. E., and Wolf-Gladrow, D.: CO2 in seawater: equilibrium, kinetics, isotopes, 65, Gulf Professional Publishing, 2001.
 - Zeebe, R. E., and Sanyal, A.: Comparison of two potential strategies of planktonic foraminifera for house building: Mg2+ or H+ removal?, Geochimica et Cosmochimica Acta, 66, 1159-1169, 2002.
- Zeebe, R. E., Wolf-Gladrow, D. A., Bijma, J., and Hönisch, B.: Vital effects in foraminifera do not compromise the use of $\delta 11B$ as a paleo-pH indicator: Evidence from modeling, Paleoceanography, 18, 2003.
 - Zeebe, R. E.: Stable boron isotope fractionation between dissolved B(OH)3 and B(OH)4–, Geochimica et Cosmochimica Acta, 69, 2753-2766, https://doi.org/10.1016/j.gca.2004.12.011, 2005.